

Synthesis of Polythiophene-BaTiO₃ Nanocomposite in aqueous media and Electrophoretic Deposition of Composite Thin Film for Dielectric Applications



Name: Adnan Ullah Khan
Reg No: 2011-NUST-MS PhD-MS-E-03

This work is submitted as a MS thesis in partial fulfillment of the requirement for the degree of

(MS in Materials and Surface Engineering)

Supervisor: Dr. Amir Habib



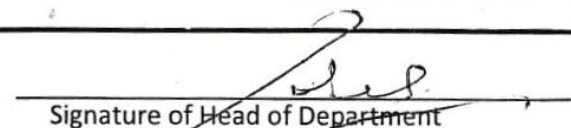
**School of Chemical and Materials Engineering (SCME)
National University of Sciences and Technology (NUST)
H-12, Islamabad, Pakistan.**

National University of Sciences & Technology**MASTER'S THESIS WORK****Formulation of Guidance and Examination Committee**

Name: ADNAN ULLAH KHAN Regn No. 2011-NUST-MSPHD-MS-E-03
 Department: Materials Engg. Specialization: Materials & Surface Engg.
 Credit Hours Completed: 24 GPA / CGPA: 3.44

Course Work Completed

S. No	Code	Title	Core / Elective	CH	Grade
1	MS-851	Surface Engineering and Characterization	Core	3	A
2	MS-821	Mechanical Behaviour of Materials	Core	3	B
3	MS-811	Materials Thermodynamics	Core	3	B+
4	MS-812	Phase Transformation and Microstructure	Elective	3	B
5	MS-880	Corrosion and Protection	Elective	3	B+
6	MS-855	Nano Materials and Nanoprocessing	Elective	3	B
7	MS-872	Composite Materials	Elective	3	A
8	MS-854	Characterization of Materials	Elective	3	B+

Date 17/06/2013Student's Signature **Thesis Committee Members:**Supervisors Name: Dr. AMIR HABIBSignature: **Members:**1. Name: Dr. IFTIKHAR HUSSAIN GulDepartment: SCMESignature: 2. Name: Dr. AHMAD NAWAZDepartment: SCMESignature: Date 20 Jun 2013Signature of Head of Department **APPROVAL**Dean / PrincipalDate: 20 Jun 2013**Distribution**

- 1 x copy to Exam Branch, HQ NUST
- 1 x copy to PGP Dte, HQ NUST
- 1 x copy to Exam Branch, Respective Institute



National University of Sciences & Technology (NUST)

FORM TH-4

MASTER'S THESIS WORK

We hereby recommend that the dissertation prepared under our supervision by

Regn No & Name: 2011-NUST-MS PhD-MS-E-03 Adnan Ullah Khan

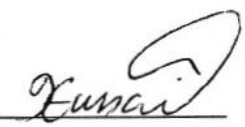
Title: Synthesis of Polythiophene-BaTiO₃ Nanocomposite in Aqueous media and Electrochromic Deposition of Composite Thin Film for Dielectric Applications.

Presented on: 18-08-2015 at: 1000 hrs in SCME Seminar Hall


Be accepted in partial fulfillment of the requirements for the award of Masters of Science degree in Materials & Surface Engineering.

Guidance & Examination Committee Members


Name: Dr Iftikhar Hussain Gul

Signature: 

Name: Dr Ahmad Nawaz

Signature: 

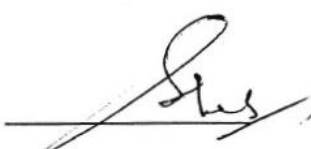
Name: Dr Erum Pervaiz (External)

Signature: 

Supervisor's Name: Dr Amir Habib

Signature: 

Dated: 28/8/2015



Head of Department

Date 2/9/2015




Dean/Principal

Date 2/9/15

Certificate for Plagiarism

It is certified that PhD/M.Phil/MS Thesis Titled "Synthesis of Polythiophene-BaTiO₃ Nanocomposite in Aqueous media and Electrophoretic Deposition of Composite Thin Film for Dielectric Applications" by Regn No 2011-NUST-MS PhD-MS-E-03 Adnan Ullah Khan has been examined by us. We undertake the follows:

- a. Thesis has significant new work/knowledge as compared already Published or are under consideration to be published elsewhere. No sentence, equation, diagram, table, paragraph or section has been copied verbatim from previous work unless it is placed under quotation marks and duly referenced.
- b. The work presented is original and own work of the author (i.e. there is no plagiarism). No ideas, processes, results, or words of others have been presented as author own work.
- c. There is no fabrication of data or result which have been compiled/analyzed.
- d. There is no falsification by manipulating research materials, equipment, or processes, or changing or omitting data or result such that the research is not accurately represented in the research record.
- e. The thesis have been checked using TURNITIN (copy of originally report attached) and found within limits as pre HEC Plagiarism Policy and instructions issued from time to time.


MS Thesis Supervisor
(Dr Amir Habib)
28 Aug 2015

Thesis Submission Certificate

It is to certify that work in this thesis has been carried out by **Adnan Ullah Khan** and completed under my supervision in School of Chemical and Materials Engineering, National University of Sciences and Technology, H-12, Islamabad, Pakistan.

Supervisor
Dr Amir Habib

Submitted Through

Principal/Dean
School of Chemical and Materials Engineering
National University of Sciences and Technology

ACKNOWLEDGEMENT

First of all, I am grateful to The Almighty ALLAH for establishing me to complete my research work.

I present my sincere gratitude to my research supervisor Dr. Amir Habib for his expert, sincere and valuable guidance and encouragement extended to me. I am fully indebted to him for his understanding, wisdom, patience, enthusiasm and for pushing me farther than I thought I could go. My gratitude also extends towards my Co-supervisor Dr. Adeel. Their support and suggestions throughout the research work has led me to complete my research work.

I wish to express my sincere thanks to Prof Dr. Muhammad Mujahid (Principal School of Chemical and Materials Engineering SCME) and to Prof Dr Muhammad Shahid (HOD Materials engineering SCME) for providing me all the necessary facilities.

I take this opportunity to record my sincere thanks to my friends for helping me survive all the stress and not letting me give up.

Adnan Ullah Khan

DEDICATION

To my Parents and Friends

ABSTRACT

Processibility and dielectric properties of Barium Titanate (BaTiO_3), which is an excellent dielectric material, were enhanced by preparing its composite with conducting polythiophene(PTh) polymer. Composite, possessing polythiophene encapsulated Barium Titanate nanoparticles was prepared via heterogeneous oxidative polymerization of thiophene by copper (II) Sulphate in presence of BaTiO_3 nanoparticles with average size of 60nm. The purpose of using BaTiO_3 nanoparticles of 60nm size was to increase BaTiO_3 -Pth interphase and reduce number of voids and pores to get uniform dielectric behavior. The morphology of the Composite was studied by SEM, proving the presence of Core-shell structures. FTIR and XRD confirmed the formation of composite. Dielectric loss and dielectric constant of pressed pellets of composites with different BaTiO_3 -PTh ratios were measured by LCR meter. Coating of polythiophene on BaTiO_3 nanoparticles decreased the dielectric loss from 0.04 for pure BaTiO_3 up to 0.008 with 40% PTh at 1.2 MHz. Maximum Dielectric constant of 30 at low frequency for 20%polythiophene and 80% BaTiO_3 was observed. Moreover, the resultant composite shows quite stability in dielectric properties in the range of 10 GHz to 15GHz. Electrophoretic deposition technique was employed to form thin films of polythiophene coated BaTiO_3 nanoparticles on conducting substrates (ITO, Cu, Stainless steel). Uniform films with average roughness of 9 nm by AFM and thickness of 360 nm by SEM and AFM were observed. Chemical nature of films was confirmed by FTIR and EDS.

TABLE OF CONTENTS

ACKNOWLEDGEMENT	iii
DEDICATION	vii
ABSTRACT	viii
List of Figures:	xi
List of Tables:	xiii
List of Abbreviations:	xiii
1 Introduction	1
2 Literature Review	3
2.1 Dielectric Materials	3
2.1.1 What are Dielectrics	3
2.1.2 Inorganic Dielectric Materials	5
2.1.3 Barium Titanate	7
2.1.4 Polymeric Dielectric Materials	13
2.1.5 Polythiophene	15
2.1.6 Dielectric Polymer Composites	17
2.1.7 Dielectric Nanocomposites	17
2.1.8 Barium Titanate –Polymer Nanocomposites	18
2.1.9 Barium Titanate Thinfilms	19
3 Synthesis Methods and Characterization Techniques	21
3.1 Synthesis methods of Barium Titanate	21
3.1.1 Solid State method for Barium Titanate Synthesis	21
3.1.2 Chemical routes for Barium Titanate Synthesis	21
3.2 Synthesis Methods of Polythiophene	23
3.2.1 Chemical Synthesis	23
3.2.2 Electrochemical Synthesis	24
3.3 Electrophoretic Deposition	24
3.4 CHARACTERIZATION TECHNIQUES	25
3.4.1 FTIR Spectroscopy	25

3.4.2	X-ray Diffraction (XRD)	27
3.4.3	Scanning Electron Microscope (SEM).....	29
3.4.4	Atomic Force Microscope (AFM)	30
3.4.5	LCR Meter	31
4	Experimental Work	32
4.1	Barium Titanate Synthesis	32
4.2	PTh/ BaTiO ₃ Composite Synthesis.....	32
4.3	Electrophoretic Thinfilm Deposition of PTh/BaTiO ₃	33
4.3.1	Substrates Used for Electrophoretic Deposition.....	33
4.3.2	Cleaning of Substrate	33
4.3.3	Solvents used for Suspension Preparation	33
4.3.4	Electrophoretic Deposition of Thinfilm.....	34
4.3.5	Vacuum Drying	35
4.3.6	Annealing.....	35
5	Results and Discussion	36
5.1	Morphology of composite particles.....	36
5.2	Chemical structure of composite	37
5.2.1	Fourier Transform Infrared Spectroscopy (FTIR)	37
5.2.2	X-Ray Diffraction (XRD)	38
5.3	Electrophoretic Deposition.....	39
5.4	Dielectric Measurements	41
6	Conclusion	47
	References	48

List of Figures:

Fig. 2.1	Effective contribution of different polarization mechanisms to the permittivity	4
Fig. 2.2	P-E (Hysteresis) diagram of (a) Ferroelectric (FE) (b) Relaxor Ferroelectric (RFE) (c) Anti-ferroelectric (AFE) (d) Linear dielectrics (LD).....	6
Fig. 2.3	Perovskite structure of BaTiO ₃ : a) BO ₆ Octahedra (blue=Ba, green=oxide) b) unit cell (blue=Ba, green=oxide, red= Ti).....	8
Fig. 2.4	Phases of Barium Titanate a) Cubic b) Tetragonal c) Orthorhombic d) Rhombohedral.....	9
Fig. 2.5	Hysteresis Loop for typical ferroelectric.....	10
Fig. 2.6	Hysteresis Loop of BaTiO ₃	10
Fig. 2.7	Effect of grain size on relative permittivity of Barium Titanate.....	12
Fig. 2.8	Effect of temperature on relative permittivity of different grain size Barium Titanate.....	13
Fig. 2.9	Mechanism of formation of Polaron and Bipolaron.....	16
Fig. 2.10	Polymer –filler matrix.....	18
Fig. 2.11	SEM images of (a) BT-PC (non-modified), (b) BT-PC (modified), (c) BT-PVDF (modified) and (d) BT-PVDF (non-modified).....	19
Fig. 3.1a	(a) FT-spectrometer24 (b) Schematic diagram of Fourier Transform Infrared spectrophotometer.....	26
Fig. 3.2	Diffraction through crystal lattice.....	27
Fig. 3.3	(a) X-Ray Diffractometer STOE θ - θ (b) Schematic diagram of Diffractometer.....	28
Fig. 3.4	(a) Scanning Electron Microscope (JSM 6490LA) ; (b) SEM Schematic.....	29
Fig. 3.5	(a)AFM JEOL (JSPM-5200); (b) Schematic diagram of AFM.....	30
Fig.3.6	Waynekerr impedance analyzer 6505.....	31
Fig. 4.1	Schematic drawing of core shell formation process.....	33
Fig. 4.2	Suspension of composite in Propanol-Water Mixture	34
Fig. 4.3	Schematic diagram of cell for Electrophoretic Deposition.....	35
Fig. 5.1	SEM micrographs of BaTiO ₃ -PTh Nanoparticles.....	36

Fig. 5.2	SEM micrographs of BaTiO ₃ -PTh Nanocomposite.....	37
Fig. 5.3	FTIR spectrum of Barium Titanate(BT), Polythiophene(PTh) and PTh/BT Composite(BTPTH).....	38
Fig. 5.4	XRD patterns of Polythiophene(PTh) and PTh/BaTiO ₃ nanoparticles.....	39
Fig. 5.5	Schematic drawing of process and mechanism of EPD.....	40
Fig. 5.6	SEM micrographs of thin films: (a) Surface Morphology, (b) Film thickness.....	40
Fig. 5.7	AFM images of thin film: (a) 3D surface topography, (b) surface roughness.....	41
Fig. 5.8	Comparison of Dielectric constant of press pellets (X=%age of polythiophene).....	42
Fig. 5.9	Comparison of Dielectric loss tangent (tanδ) of press pellets (X = %age of polythiophene).....	43
Fig. 5.10	Comparison of Dielectric loss (ε'') of press pellets (X = %age of polythiophene).....	44
Fig. 5.11	Comparison of AC conductivity (σ _{AC}) of press pellets (X = %age of polythiophene).....	45

List of Tables:

Table 2.1	Dielectric constants of some useful inorganic dielectric materials.....	6
Table 2.2	Effect of synthesis method on dielectric constant.....	10
Table 2.3	Polymers with dielectric constants commoly used in capacitors.....	13
Table 2.4	Breakdown field strength of common polymers.....	14
Table 3.1.	Difference between Electrophoretic and Electrolytic Deposition.....	22

List of Abbreviations:

AFE	Anti Ferroelectric
AFM	Atomic Force microscopy
BTPth	Barium Titanate Polythiophene
BT	Barium Titanate
DC	Direct Current
DD	Double Distilled
DRAM	Dynamic Ram Access Memory
EPD	Electrophoretic Deposition
FE	Ferroelectric
FET	Field Effect Transistor
FTIR	Fourier Transform Infra Red Spectroscopy
HCl	Hydrochloric Acid
ITO	Indium Tin Oxide
LCR	Inductance conductance Resistance
LD	Linear Dielectric
MLCC	Multi-Layer Cermaic Capacitor
PC	Polycarbonate
PMMA	Polymethyl Metha Acrylate
PTh	PolyThiophene
PVDF	Poly Vinylidene Flouride
RFE	Relaxor Ferroelectric

SDS	Sodium Dodecyl Sulphonate
SEM	Scanning Electron Microscope
SRAM	Static Random Access Memory
SS	Stainless Steel
XRD	X-Ray Diffraction

1 INTRODUCTION

Dielectric materials are used to store electrical energy in the form of charge separation when polarized by an external electric field. Ceramic based inorganic dielectric materials have traditionally been used in ceramic capacitors for pulse power application and in Field Effect transistors. Several materials have been used as dielectric materials such as BaTiO₃, PbTiO₃, PbNb₂O₆, PLZT and SrTiO₃[1]. In spite of having high dielectric constant, ceramic capacitors have low break down field strength, which results in low energy density. Additionally, processing of ceramics for use in capacitors and FETs at room temperature is difficult[2]. To overcome this problem, Polymer/ceramic nanocomposite is the best option. Polymers have low permittivity but high breakdown field strength, low dielectric loss and high mechanical characteristics. These characteristics of polymers can be combined with ceramics in a composite system. Not all the properties but a compromise between the two will be possible. Use of nanoceramics increases the polymer-inorganic interphase which results better and homogeneous characteristics. To choose ceramic filler, the one with high dielectric constant should be chosen as the polymer matrix reduces the overall dielectric constant of the composite. Barium Titanate(BaTiO₃) is the most efficient dielectric material whose dielectric constant ranges up to 1700[1]. Many Barium Titanate(BT)-Polymer nanocomposites have been investigated. Some of them are BaTiO₃-polyimide[3], BaTiO₃-polyaniline[4], BaTiO₃-PVDF, BaTiO₃-epoxy[5]. The resultant composites have good processibility, high breakdown field strength and high dielectric constant. Dang et al reported about BaTiO₃/polyimide nanocomposite films with high dielectric constant (~20), high breakdown strength (~67 MV) and high thermal stability by in-situ polymerization process. A very thin polymer layer (about 5 nm) was coated on the surface of BaTiO₃ nanoparticles to form a core-shell-like structure, which can guarantee homogeneous dispersion of the BaTiO₃ particles in the Polyimide matrix[3]. Moreover, for BaTiO₃/epoxy composites thin film, dielectric constant of about 40 at 1 kHz and loss factor of less than 0.035 over a wide range of frequency has been achieved by Liang et al. [5]

In this research work, composite of Barium Titanate(BaTiO_3) /polythiophene(PTh) is prepared by encapsulating BaTiO_3 with PTh. To the best of our knowledge coating of polythiophene on BaTiO_3 has not yet been reported in the literature. The purpose of this research work was to enhance the processability of BaTiO_3 on addition of PTh and also studied the effect of BaTiO_3 percentage on dielectric properties of Polythiophene. In our work, composites with different BaTiO_3 -PTh ratio were synthesized by in-situ oxidative polymerization of thiophene[6] in the presence of BaTiO_3 nanoparticles with average size of 60nm. The resultant composite was found fruitful as addition of BaTiO_3 into PTh drastically enhanced the dielectric constant. The two extreme percentages of BaTiO_3 and PTh have all the composition between them where desired dielectric properties containing composite can be selected. Secondly, a homogenous and uniform thin film was prepared through Electrophoretic Deposition technique.

The morphology of the composite is studied by Scanning electron microscopy (SEM). SEM analysis confirmed the presence of core-shell structures of the BaTiO_3 -PTh composite. FTIR and XRD confirmed the formation of composite. Dielectric loss tangent and dielectric constant of pressed pellets of composites with different ratio of BaTiO_3 and polythiophene is studied by LCR meter.

Electrophoretic deposition technique is employed to form thin film of polythiophene coated BaTiO_3 nanoparticles on various conducting substrates such as ITO, Cu and Stainless steel. Film thickness is confirmed by atomic force microscopy (AFM) and SEM respectively.

2 LITERATURE REVIEW

2.1 DIELECTRIC MATERIALS

Dielectric Materials are widely being used in storage devices, power systems, pulse power applications and Field Effect Transistors[1, 7] .Capacitor is a passive component of electronic devices and is used in these applications to store energy. In addition to advancement of active electronics there is a need of capacitors which can store more energy and can deliver it rapidly. The one way to increase the energy density is by using efficient dielectric materials [8].

2.1.1 WHAT ARE DIELECTRICS

Dielectric materials are insulators which store electrical energy when polarized by an external electric field in the form of charge separation [8].

Relative permittivity (ϵ_r) or dielectric constant expresses the ability of a dielectric materials to store charge. Dielectric constant of a material is measured in the form of dielectric displacement D when electric field of strength E is applied. Mathematically:

$$\epsilon_r = \left[\frac{\partial D}{\partial E} \right]_{E=0} \quad \text{Equation (2.1)}$$

Dielectric Displacement is related to polarization (P) as shown in equation below;

$$D = E + 4\pi P \quad \text{Equation (2.2)}$$

So, permittivity can be expressed as

$$\epsilon_r = E + 4\pi \frac{\partial P}{\partial E} \quad \text{Equation (2.3)}$$

The Different types of polarization mechanisms are:

- **Electronic Polarization**: stretching or shifting of electronic cloud around a nucleus.
- **Ionic Polarization**: separation of oppositely charge species by electric field.
- **Dipole Polarization**: alignments of dipole species along the applied electric field
- **Space Charge Polarization**: polarization due to orientation of charged defects in the material in response to external electric field.

The total polarization is the sum of all these polarization and collectively contributes to the permittivity. At low frequency all mechanisms contribute except electronic polarization which is effective only at higher frequencies where others are not as shown in Figure 2.1[9].

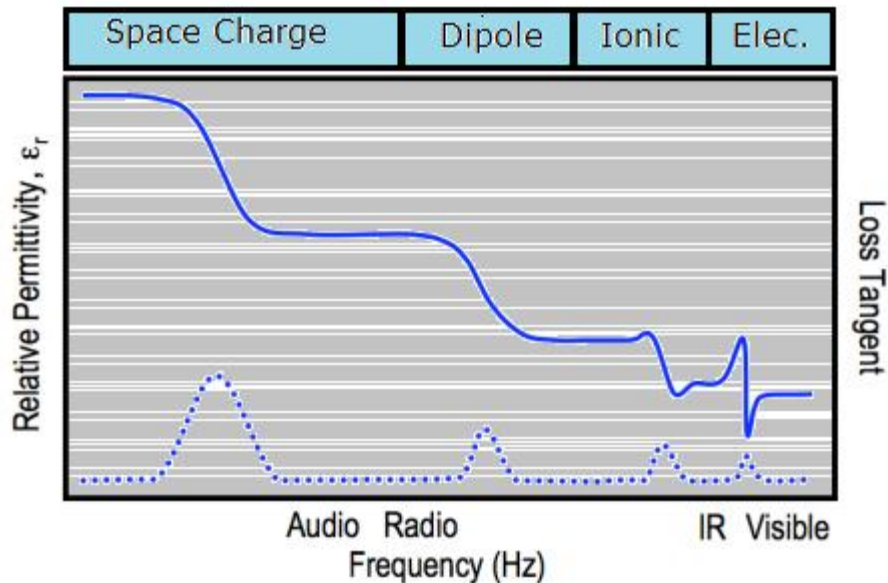


FIG. 2.1 Effective contribution of different polarization mechanisms to the permittivity

The complex permittivity of a dielectric can be written as:

$$\varepsilon^* = \varepsilon' - j \varepsilon'' \quad \text{Equation (2.4)}$$

Here ε' is real and ε'' is imaginary part of the complex permittivity. Imaginary part of the complex permittivity is also called dielectric loss of the material. Dielectric loss of the material can also be expressed in terms of loss tangent which is equal to:

$$\tan \delta = \frac{\epsilon''}{\epsilon'} \quad \text{Equation (2.5)}$$

Capacitance of a parallel plate capacitor depends on area of the plate A and thickness d of the dielectric material between the two plates. Mathematically it can be expressed as:

$$C = \epsilon_o \epsilon_r A/d \quad \text{Equation (2.6)}$$

Energy stored by a capacitor depends on breakdown voltage V_{bd} :

$$W = \frac{1}{2} CV_{bd}^2 \quad \text{Equation (2.7)}$$

2.1.2 INORGANIC DIELECTRIC MATERIALS

There are numbers of inorganic dielectric materials which are investigated till the day. Different types of inorganic dielectric materials are classified as [10]:

- Ferroelectric (**BaTiO₃**, **PbTiO₃** etc)
- Relaxor Ferroelectric (**PbZrO₃**, **LaTiO₃**, **LaZrO₃** etc)
- Anti-ferroelectric (**PbZrO₃**)
- Linear dielectrics (**Glass**, **Al₂O₃**)

Ferroelectric materials are those materials which show spontaneous polarization when subjected to electric field. While Anti ferroelectric materials are those which have two sub-lattices and when subjected to electric field, polarize spontaneously in anti parallel direction. Linear dielectrics are with constant permittivity and in case of relaxor ferroelectrics they used to have domains of the order of nanosize. Below Fig 2.1 shows the P-E diagrams of all four kinds of dielectrics [10].

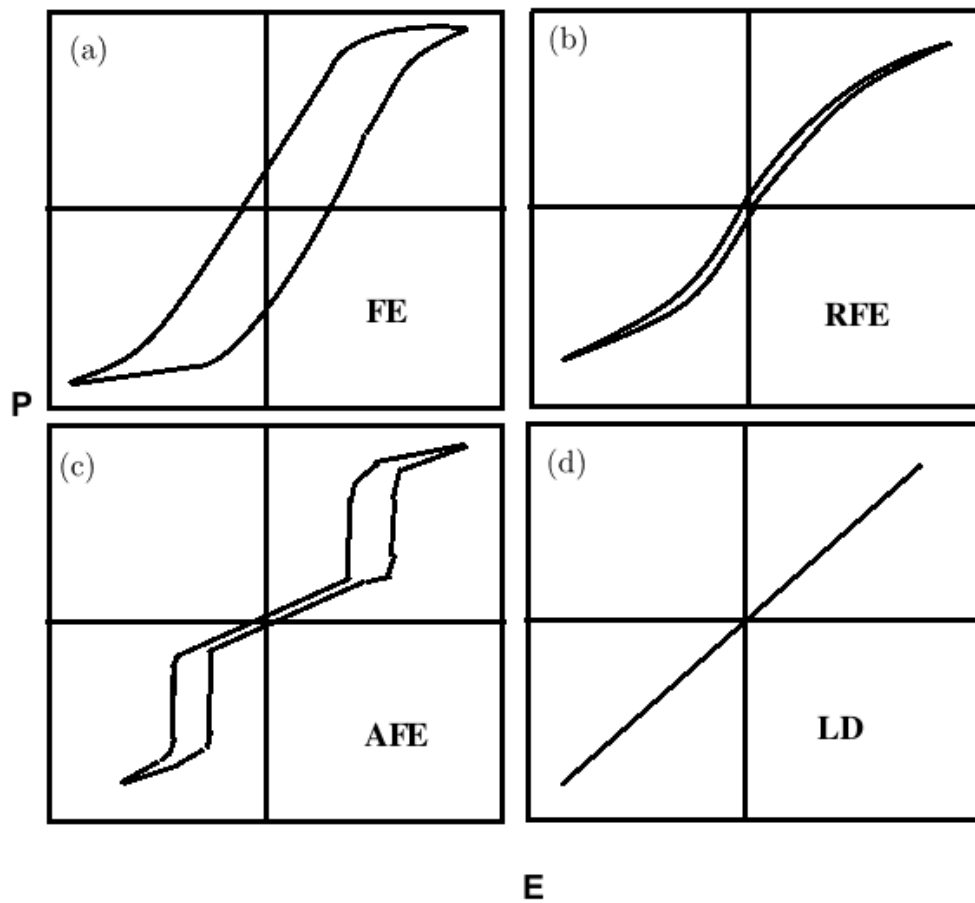


Fig. 2.2 P-E (Hysteresis) diagram of (a) Ferroelectric (**FE**) (b) Relaxor Ferroelectric (**RFE**) (c) Anti-ferroelectric (**AFE**) (d) Linear dielectrics (**LD**)

Ceramic capacitors have high dielectric constant but low breakdown field strength. Thus results low energy density. In addition, their manufacturing is difficult. Below is shown the Table 2.1 of different inorganic dielectrics with their permittivity values.

Table 2.1 Dielectric constants of some useful inorganic dielectric materials [1].

Composition	Dielectric permittivity
BaTiO ₃	1,700
PMN-PT (65/35)	3,640
PbNb ₂ O ₆	225
PLZT (7/60/40)	2,590
SiO ₂	3.9
Al ₂ O ₃	9
Ta ₂ O ₅	22
TiO ₂	80
SrTiO ₃	2,000
ZrO ₂	25
HfO ₂	25
HfSiO ₄	11
La ₂ O ₃	30
Y ₂ O ₃	15
α -LaAlO ₃	30
CaCu ₃ Ti ₄ O ₁₂	~60,000
La _{1.8} Sr _{0.2} NiO ₄	~100,000

2.1.3 BARIUM TITANATE

Barium Titanate is a ferroelectric material whose ferroelectricity was first discovered in 1945 in Russia and then in 1946 in United States independently. Vul et al. reported non-linear behavior of permittivity in Barium Titanate when subjected to electric field but they did not classify BaTiO₃ as ferroelectric [11]. After analyzing the work of Megaw and on observation of hysteresis in Barium Titanate they concluded that it was a ferroelectric material [12]. Since the discovery of ferroelectricity in Barium Titanate, it is widely being used in Passive electronics as energy storage and in Field effect transistors.

2.1.3.1 PEROVSKITE STRUCTURE

Barium Titanate belongs to a family called “perovskite” whose general formula is ABO₃. The name perovskite is taken from the mineral “Perovskite”, CaTiO₃. ABO₃ type of crystalline structure in primitive cubic form has A-cation at the corner (mono,di,tri-valent), B-cation in the centre of cube (penta,tetra,tri-valent) and O-oxygen anion in the face centre. In Barium Titanate

(BaTiO₃) A is Barium and B is Titanium. There are two approaches to consider perovskite structure of Barium Titanate. It may be considered as 3-D array of BO₆ in the form of octahedral (Fig. 2.3a) or can be dealt as cubic closed packed array of A and O where B is located at the interstices (Fig. 2.3 b)[13-15].

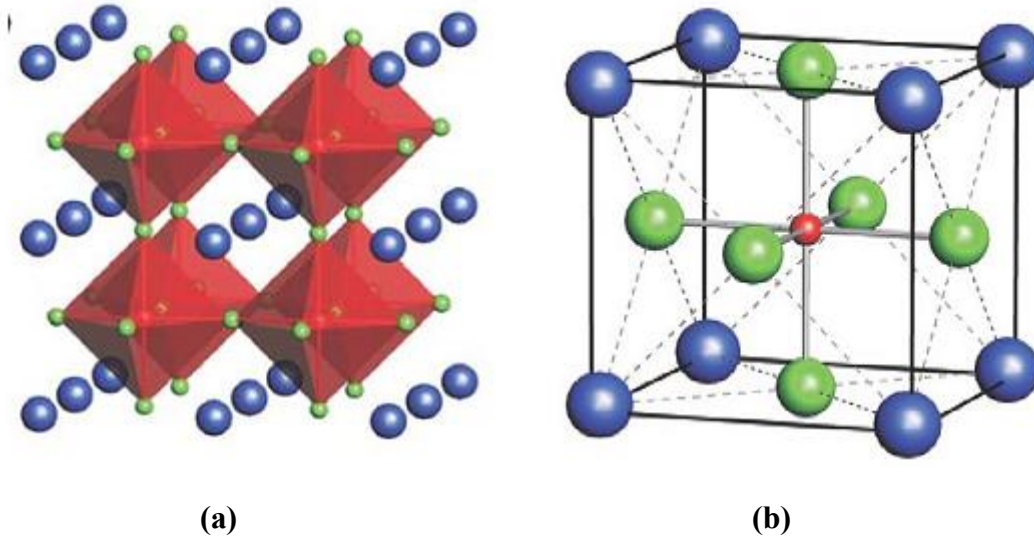
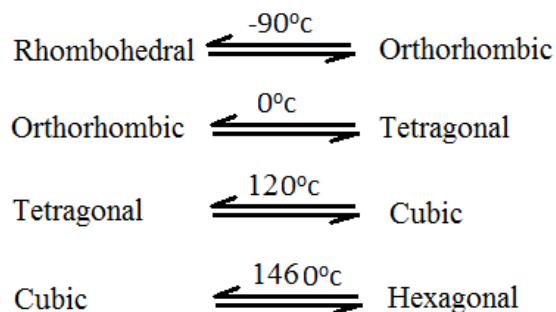


Fig. 2.3 Perovskite structure of BaTiO₃: **a)** BO₆ Octahedra (blue=Ba, green=oxide) **b)** unit cell (blue=Ba, green=oxide, red= Ti)[16]

Barium Titanate exists in five crystalline forms at different temperature ranges. Different crystalline forms with their transition temperature are given below:



Below are the figures that show different crystallographic changes in perovskite structure of Barium Titanate[11].

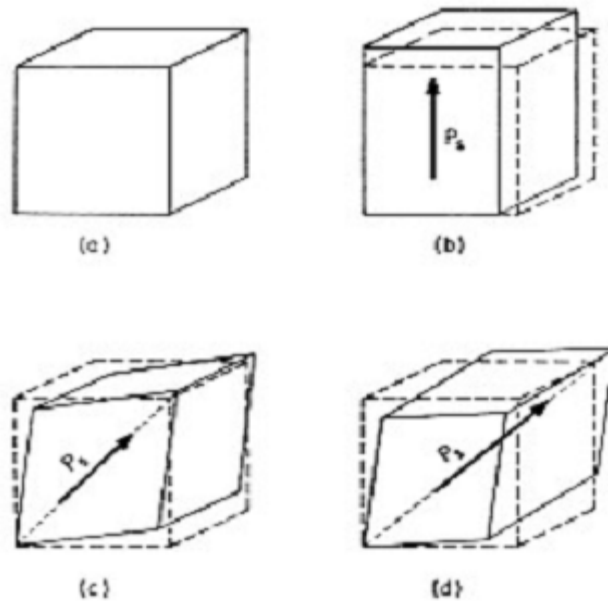


Fig. 2.4 Phases of Barium Titanate **a)** Cubic **b)** Tetragonal **c)** Orthorhombic **d)** Rhombohedral

The temperature at which tetragonal to cubic phase transition takes place is called as Curie temperature. Curie temperature of Barium Titanate is 120°C. This is the temperature above which primitive perovskite cubic structure is stable.

2.1.3.2 FERROELECTRICITY

Barium Titanate is a ferroelectric material and shows spontaneous polarization. This spontaneous polarization is due to non-centrosymmetry in the unit cell which creates dipole moment. Orientation of these dipoles in the same direction generates small polarized regions called as domains. Above Curie temperature, Barium Titanate behaves as paraelectric due to centrosymmetric cubic structure. But below this temperature it exists in non-centrosymmetric tetragonal phase thus spontaneously polarized electric domains are generated. When ferroelectric Barium Titanate is kept under electric field, change in polarization is observed. Below is shown effect of electric field on polarization (Hysteresis Loop) [9, 11, 15].

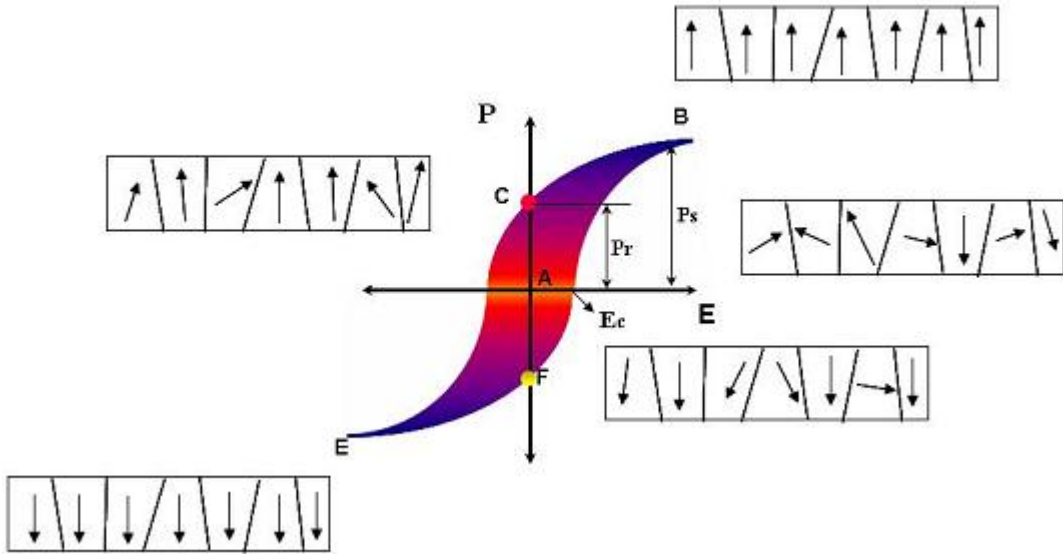


Fig. 2.5 Hysteresis Loop for typical ferroelectric

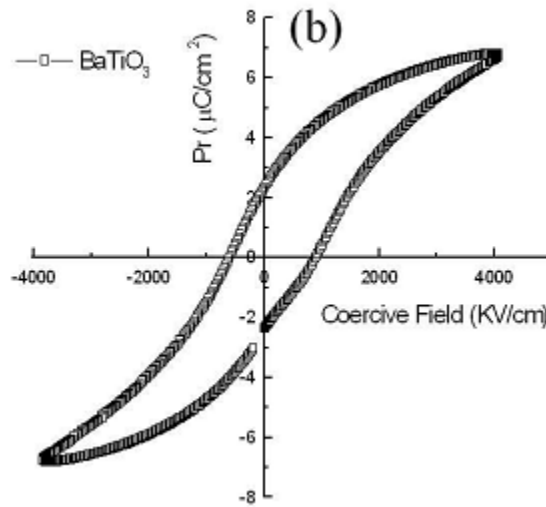


Fig. 2.6 Hysteresis Loop of BaTiO₃ [17]

When electric field is applied, initially those domains which are not oriented along the field reverse their direction. In hysteresis loop, it shows a linear behavior. When electric field becomes high, saturation occurs. But when electric field is decreased to zero, still polarization is

observed in the material known as remnant polarization, P_R . While value of polarization at saturation point is called spontaneous polarization, P_S . The E_c is the coercive field, required to nullify the polarization [11-15].

2.1.3.3 DIELECTRIC PROPERTIES

Since the discovery of ferroelectricity in Barium Titanate, it is the most demanding dielectric material in electronic industries due to high value of dielectric constant. Its dielectric constant changes with synthesis route, density, crystalline nature and particle size[7]. Temperature, frequency and dopants are some other factors which affect the dielectric behavior.

Various researchers reported the effect of synthesis route on dielectric constant of barium Titanate. Some of them are shown below in Table 2.2.

Table 2.2 Effect of synthesis method on dielectric constant.

Synthesis Route	Dielectric Constant	Frequency	Reference
Sol-gel method	1300	1kHz	M Cernea [18]
Hydrothermal method	2000	1kHz	Boulos et al. [19]
Co-precipitation method	665	10kHz	Testinion et al. [20]
Polymeric Precursor method	1700	1kHz	V. Vinothini et al.[21]

Usually in ferroelectrics, it has been observed that by decreasing the grain size up to 1 micron, dielectric constant increases. But further reduction causes a decrease in dielectric permittivity [22].It has been reported that the critical size for ferroelectric to show polarization is on the order of 30 unit cells. The reason is that by decreasing the size up to limit, paraelectric/ferroelectric transition temperature needed would be below 0 K [23].

Dielectric constant of Barium Titanate increases starting from 5 micron with average size of 1500 up to 6000 for 1 micron [24, 25]. For larger than 5 micron grain size, dielectric constant up to 2000 has been reported [25]. Arlt et al. [26] reported the effect of grain size on the permittivity of polycrystalline materials. For this purpose they prepared Barium Titanate particle of different sizes between 0.3 and 50 micron. A graph between permittivity at room temperature and average grain size plotted by Arlt et al. is shown below in Fig. 2.7.

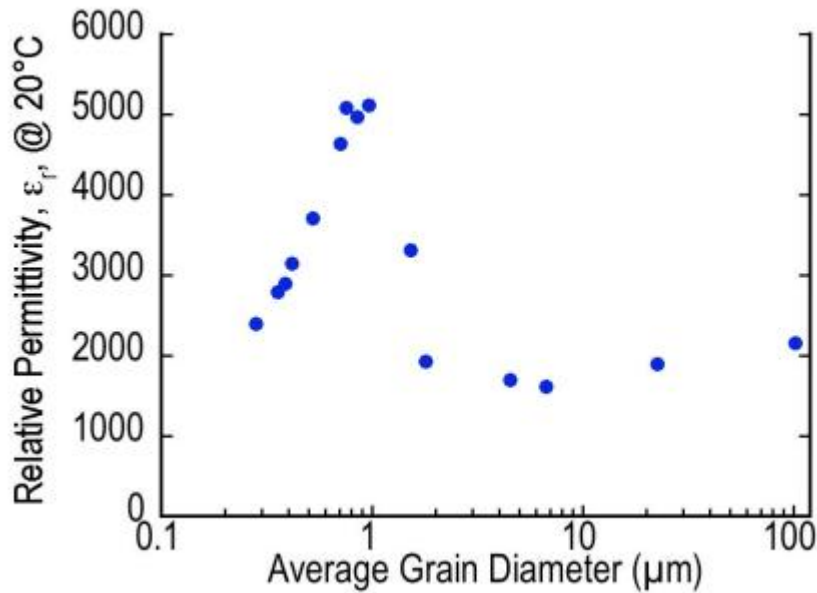


Fig. 2.7 Effect of grain size on relative permittivity of Barium Titanate.

Below 100nm size, the probability of finding tetragonality in Barium Titanate reduces due to lowering of phase transition temperature for cubic/tetragonal. Different values of critical particle size, below which Barium Titanate does not show ferroelectricity and only exists in cubic phase (paraelectric), has been reported which ranges up to 40 nm [27].

Effect of temperature on relative permittivity for different grain size has been reported by Frey et al. [22]. Below is shown the graph Fig. 2.8.

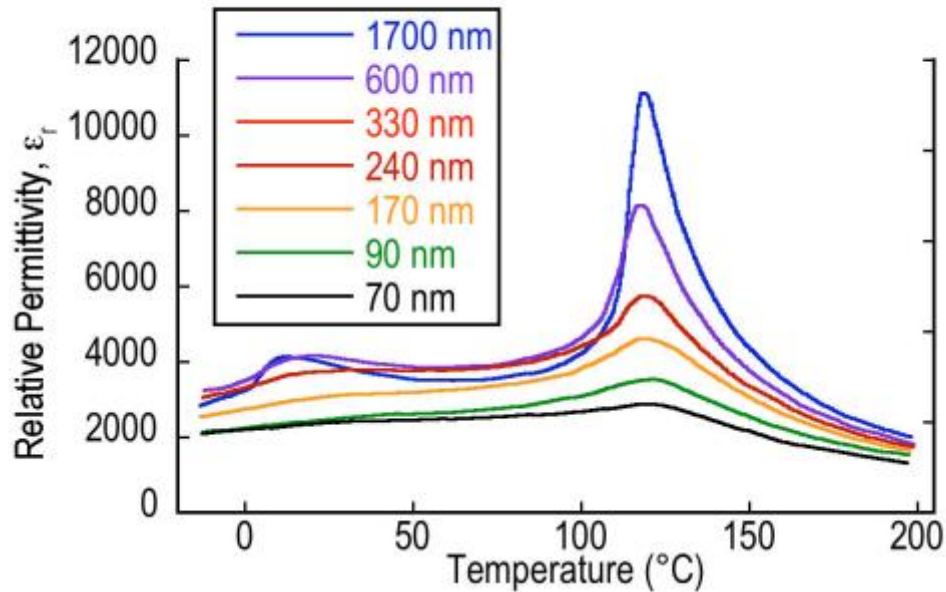


Fig. 2.8 Effect of temperature on relative permittivity of different grain size Barium Titanate[22]

2.1.4 POLYMERIC DIELECTRIC MATERIALS

Polymers are macromolecules with repeating units called monomers. Polymers are known for their ease to synthesize, process to any form, flexibility, strength and stable in harsh environment with wide range of properties finds its application in almost any field. In the same way it finds its way in passive electronics due good isolative properties and easy to manufacture with good mechanical strength. There are numbers of polymers which are being used in capacitors both as high-k and low-k dielectric materials. Some of them are listed below with the values of dielectric constants [1].

Table 2.3 Polymers with dielectric constants commonly used in capacitors[1]

Polymer	Dielectric permittivity
Nonfluorinated aromatic polyimides	3.2-3.6
Fluorinated polyimide	2.6-2.8
Poly(phenyl quinoxaline)	2.8
Poly(arylene ether oxazole)	2.6-2.8
Poly(arylene ether)	2.9
Polyquinoline	2.8
Silsesquioxane	2.8-3.0
Poly(norborene)	2.4
Perfluorocyclobutane polyether	2.4
Fluorinated poly(arylene ether)	2.7
Polynaphthalene	2.2
Poly(tetrafluoroethylene)	1.9
Polystyrene	2.6
Poly(vinylidene fluoride-co-hexafluoropropylene)	~12
Poly(ether ketone ketone)	~3.5

Polymers have high break down field strength, low dielectric loss and easy to process. But the disadvantage is that they have low dielectric constant.

Breakdown field strength is the ability of an insulating material to with stand high electric field beyond which it become conductor. Polymers are the good candidates having high breakdown field strength. Some of them are listed in table 2.4. The reasons behind this breakdown are the three mechanisms viz Ionization, intrinsic mechanism and thermal mechanism [28, 29].

Table 2.4 Breakdown field strength of common polymers [30].

Polymer	Dielectric Strength (V/μm)
Polyethylene (LD)	200
Polyethylene (HD)	200
Polyethylene (XL)	220
Polypropylene (Biaxially oriented)	200
Polystyrene	200
Polytetrafluoroethylene	88-176
Poly(vinylidene fluoride)	10.2
Polycarbonate	252
Polyester	300
Polyimide	280
Epoxy resin	25-45

2.1.5 POLYTHIOPHENE

Polythiophene being conducting finds its applications in electronic industry such as in photovoltaic cells, electrode materials in pseudo capacitors, supercapacitors, batteries, diodes and also used as chemical sensors [31-33]. Polythiophene consists of sulphur based heterocyclic thiophene monomers. It is insulator in pure form. Its conductivity can be set from semiconductor to complete conductor through doping process. The presence of conjugated pi-backbone makes it conducting when electron is added or removed from this backbone. Due its conductivity it is also named as synthetic metals [34].

Polythiophene is the most efficient conducting polymer due to its stability in p-doped state which is because of low oxidation potential. Polythiophene is an extrinsic conducting polymer as it needs oxidizing or reducing agent to make it conductive. When electron is removed it is called as p-doped and when electron is added to system it becomes n-doped. Structural changes are observed when electrons are added. For instance when electron is removed from polythiophene molecule, it generates mobile charge thus forms cation, polaron. Removal of second electron by further oxidation results the formation of bipolaron.

Structural changes occurs when it is oxidized are shown below in Fig. 2.9.

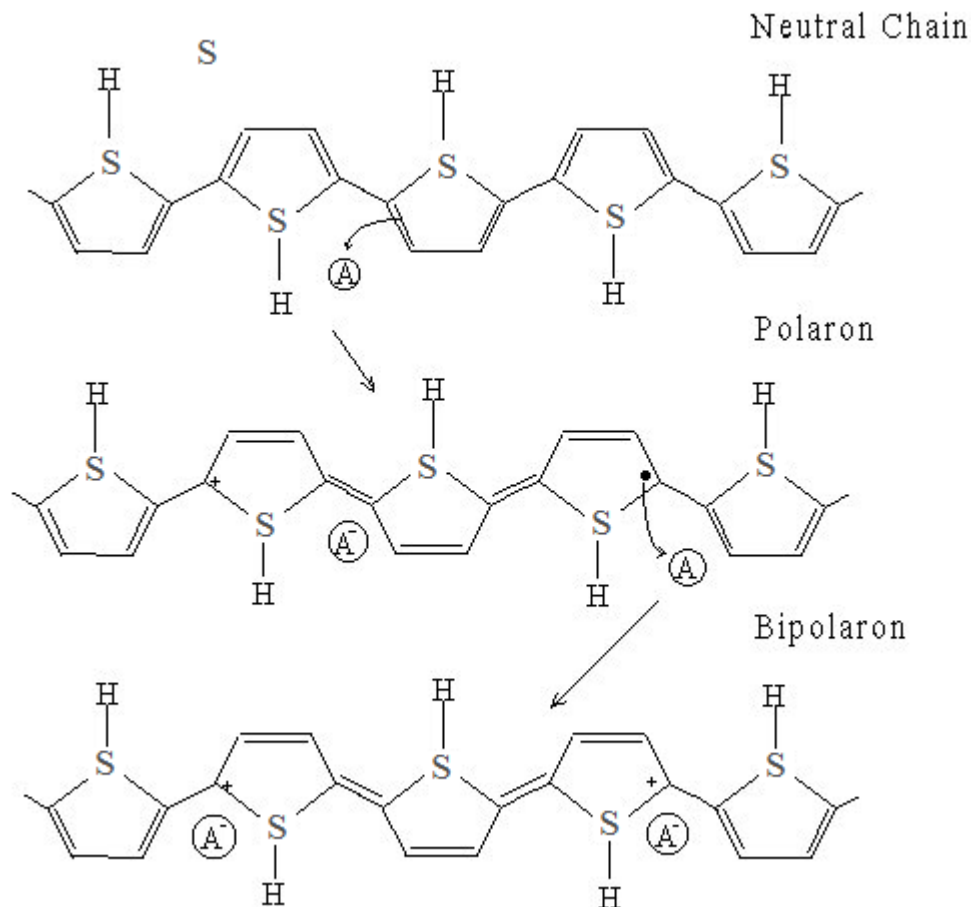


Fig. 2.9 Mechanism of formation of Polaron and Bipolaron

2.1.5.1 ELECTROCHEMICAL PSEUDOCAPACITANCE

Polythiophene and its derivatives are used as electrode material in supercapacitors due to their pseudocapacitive behavior.

Pseudocapacitors store electrical energy through reversible faradic oxidation reduction reactions by charge transfer between electrode and electrolyte. Transfer of charge is a three step mechanism that is electrosorption, redox reaction, and intercalation. Together with electric double layer, pseudocapacitor forms supercapacitor [35].

Supercapacitors are potentially being used in electronic industry where short term charge and discharge cycle is required instead of long term cycle i.e. static random access memory (SRAM), pulse laser, vehicles, cranes etc [36]. Polythiophene is best option to be used as electrode material in supercapacitors as compared to other electrode materials i.e metal oxide and conducting polymers due three properties viz (i) short charge and discharge cycle, (ii) stability in

its oxidation state (iii) and high specific capacitance [37-39]. B. Senthilkumar et al.[40] investigated the pseudocapacitive behavior of polythiophene. They first synthesized polythiophene nanoparticles and then placed on graphite strip with 30 % carbon black and 5 % PVDF to make an electrochemical electrode. Thus prepared electrode was subjected to cyclic voltammetry and results were quite fruitful. Specific capacitance of 117F/g for PTh-TRI was reported.

2.1.6 DIELECTRIC POLYMER COMPOSITES

Inorganic/ceramic dielectrics have high dielectric permittivity but low breakdown field strength which results low energy density and their processibility is very low. On the other hand polymers have low dielectric permittivity but high breakdown field strength and they are easy to be processed and shape to any form to be used as dielectric material. Both the properties of high dielectric constant of ceramics and high break down field strength of polymers can be combined by using ceramics as filler in polymer matrix. The resultant composite has high dielectric constant and high break down field strength thus results high energy density.

There are number of researches that have been carried out to make such composites where ceramics fillers were used to enhanced dielectric constant of polymer matrix. Not all the properties but a compromise between the two has been achieved due large differences among the dielectric permittivities of ceramics and polymers. Such differences results in-homogeneity and need to be resolved by working on filler-polymer interphase.

2.1.7 DIELECTRIC NANOCOMPOSITES

Dielectric constant of composites can be improved by increasing the filler-polymer interphase. Filler polymer interphase can be increased by increasing the surface area of fillers which can attain by decreasing the size of fillers.

Different theoretical models have been proposed to study the effect of filler size on dielectric constant of polymer matrix. Lewis et al. proposed that by decreasing the size of fillers upto nanometer scale, polymer-filler interphase properties dominates the individual properties [30, 41, 42]. By using the same concept, Sun et al. prepared Silica-Epoxy composite and studied the effect of silica particle size on dielectric constant. They found that by decreasing the size of silica particles from micro to nano size, dielectric permittivity and dielectric loss increases at low frequencies.

Another model by Tanaka et al. was proposed where they suggested that by modifying the surface of filler, filler-polymer matrix interphase can be enhanced and better results can be

achieved [43]. In their model they explained that for spherical fillers there are three regions of filler-polymer matrix interphase:

- (i) bonded layer: polymer is in direct contact with the surface of filler
- (ii) bounded layer: interfacial region
- (iii) and loose layer: bulk polymer

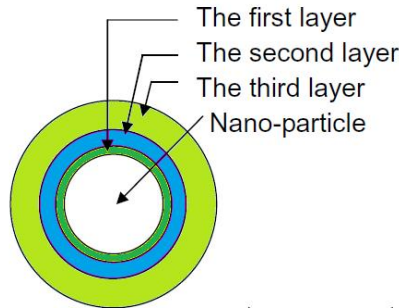


Fig. 2.10 Polymer –filler matrix

Second and third layer are more influential and affects the dielectric properties of composite more. These two layers can be modified by attaching some organic groups on the surface of filler.

2.1.8 BARIUM TITANATE –POLYMER NANOCOMPOSITES

There are number of polymers such as epoxy resins, methyl-metacrylate, polyvinylidene, polycarbonates and polyimides [44-46] are being used as matrix with Barium Titanate to enhance the overall energy density of the composite. To increase the polymer-Barium Titanate interphase interaction, surfactant such as phosphonic acid are used by many researches as suggested by Tanaka et al. [43-47].

Barium Titanate-epoxy composite for thin film capacitor was synthesized by Liang et al.[47]. A very good dispersion of Barium Titanate in epoxy resin was achieved by modifying BT nanoparticles surface with N-phenyloamine trimethoxysilane. Kim et al. reported that phosphonic acid modified BT nanoparticles well disperse in polymer matrices [46]. They choose two type of polymer matrices viz polycarbonate and PVDF-HFP to test with surface modified BT nanoparticles. Good dispersion of surface modified BT nanoparticles resulted high dielectric constant and low dielectric loss at 1MHz frequency for both polymers. Fig. 2.7 shows SEM images of thin films both modified and non-modified BT dispersed in Polycarbonate and PVDF.

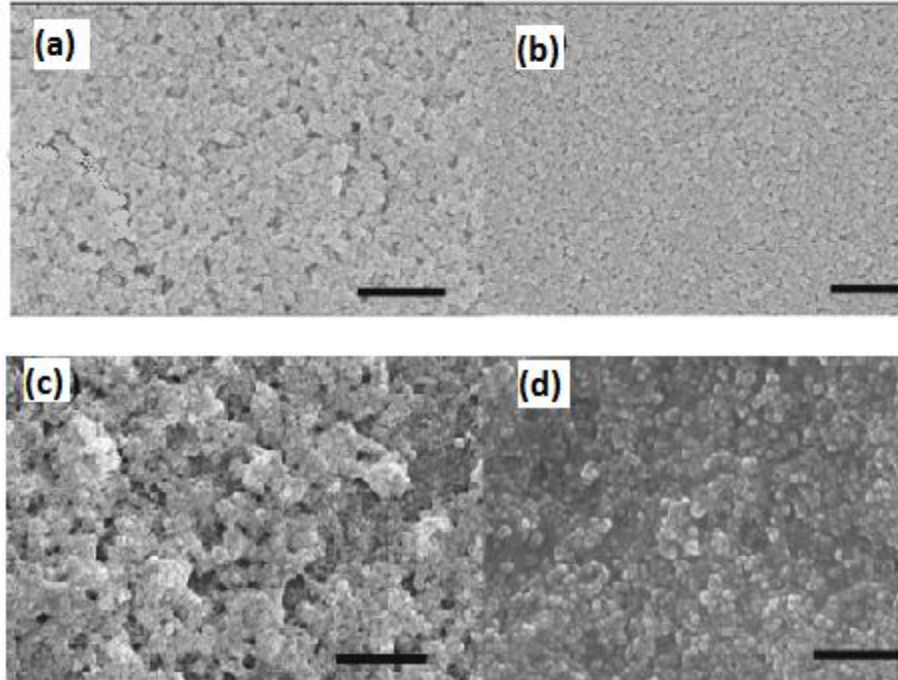


Fig. 2.11 SEM images of (a) BT-PC (non-modified), (b) BT-PC (modified), (c) BT-PVDF (modified) and (d) BT-PVDF (non-modified)

2.1.9 BARIUM TITANATE THINFILMS

Barium Titanate thinfilms have wide use in electronic industries such as in pulse power application and passive electronics i.e. Multilayered ceramic capacitors (MLCC), dynamic random access memory (DRAM) and tunable microwave devices [48-50].

First thinfilm of Barium Titanate was prepared by Feldman by vacuum deposition [51]. There are two classes of methods applied to prepare Barium Titanate thinfilms viz (i) physical methods: vapour deposition, dip coating, spin coating, spray coating and sputtering; and (ii) Chemical methods: sol-gel method and electrophoretic deposition methods [52].

With the miniaturization of electronics, the need of small size capacitors is drastically increased. For small size and high permittivity of apacitors, dielectric materials must be cast in the form of thinfilms. Barium Titanate processing is very difficult. Moreover for defects free thinfilms preparation, sintering at high temperature is required which increases the risk of reaction of substrate material with Barium Titanate. Other drawbacks are poor mechanical strength and adherence to substrates is worth mention. To overcome such problems use of polymeric materials with Barium Titanate are introduced. Low dielectric loss, high breakdown field strength and good processability of polymers combine with high dielectric permittivity of

Barium Titanate in a composite. Barium Titanate composite can be easily processed into thinfilms of nano size thickness and smooth surface.

There are many researches on thinfilm preparation of Barium Titanate nanocomposite which includes BT-epoxy resin, BT-polycarbonates, BT-PMMA, BT-PVDF and many more [44-48, 52].

3 SYNTHESIS METHODS AND CHARACTERIZATION TECHNIQUES

3.1 SYNTHESIS METHODS OF BARIUM TITANATE

Many researches have been made to synthesize Barium Titanate of different size, shape and morphology. There are many routes to prepare BT depends on initial reactants and way of reaction. These methods include:

- I. Solid state method
- II. Chemical route

3.1.1 SOLID STATE METHOD FOR BARIUM TITANATE SYNTHESIS

This method of synthesis involves mixing of BaCO_3 or BaO with TiO_2 with the help of Ball milling. After proper mixing the prepared powder is calcined at 800 to 1300 °C [53]. Solid state method has some disadvantages of agglomeration, large particle size and in homogeneity. Due to high sintering temperature Barium Titanate often reacts with substrate and cause of impurity which results poor dielectric properties.

3.1.2 CHEMICAL ROUTES FOR BARIUM TITANATE SYNTHESIS

Barium Titanate synthesized through chemical route has homogeneous composition thus results homogeneous dielectric properties. Chemical routes provide more versatility where Barium Titanate of both micro and nano size of any shape and morphology can be prepared. Different chemical routes are enlisted below.

- I. Sol-gel method
- II. Hydrothermal method
- III. Co-precipitation method
- IV. Polymeric Precursor method

3.1.2.1 SOL-GEL METHOD

Sol-gel method involves two steps mechanism: (i) sol formation by partial hydrolysis of Barium alkoxide and alkyl Titanate and subsequent condensation into oligomer, (ii) and gel formation which is done by further hydrolysis through process of aging which results cross-linking and formation of 3-D matrix. The resultant sol-gel is dried and upon pyrolysis gives crystalline Barium Titanate [54, 55].

3.1.2.2 HYDROTHERMAL METHOD

In hydrothermal method Barium Titanate crystals are synthesized at temperature greater than 25 °C and pressure higher than 100 kpa in aqueous media. Ba precursors (naitrate, chloride, hydroxide) and Ti precursors are used as starting material dissolved in aqueous media. Reaction is carried out in autoclave at autogeneous pressure which is saturated vapor pressure of the solution at specific temperature and composition. By changing the temperature, pressure and solvent, different size particles and morphology can be achieved. Hydrothermal method of synthesis is more attractive method as it involves less time and energy consumption because mixing, milling and high temperature calcination is minimized or sometime not necessary. Moreover, as the crystals are directly formed from aqueous ionic solution, nucleation and growth can be regulated to get desirable morphology and size [56].

3.1.2.3 CO-PRECIPIATION METHOD

Both Barium ion and Titanium ion is precipitated simultaneously from their ionic solution in the form of carbonates or hydroxide. These carbonates or hydroxide are converted into Barium Titanate by thermal treatment. Precipitation is generally carried out through hydrolysis at ambient temperature. Clabaugh and modified Clabaugh process[57] are known precipitation method for Barium Titanate synthesis. In this process, Barium titanyl oxalate particles are precipitated by mixing $BaCl_2$, $TiCl_4$ and oxalic acid in a suitable ratio. Then these particles are subjected to thermal treatment to get Barium Titanate particles.

3.1.2.4 POLYMERIC PRECURSOR METHOD

Polymeric precursor of both Barium and Titanium is prepared by polymerization of citric acid, metal ion and ethylene glycol. The resultant polymeric network is thermally decomposed to remove organic part and crystalline Barium Titanate particles are formed. In a well known pechini method [21], Barium citrate and Titanium citrate is first prepared and then mixed with ethylene glycol. The prepared solution is heated up to 140 °C till dark glassy mass is obtained. This black mass is first heated in oven at 200 and 300 °C and then calcined at 500 °C for 4h, at 700 °C for 3 h and for 2h at 750 °C. Agglomerates are ball milled into powder. Cubic Barium Titanate particles are formed in this method.

3.2 SYNTHESIS METHODS OF POLYTHIOPHENE

Polythiophene can be synthesized by two main methods:

- I. Chemical synthesis methods
- II. Electrochemical methods

Detail of these methods is described below.

3.2.1 CHEMICAL SYNTHESIS

Chemical synthesis methods are further categorized into (i) metal catalyzed and (ii) oxidative polymerization.

First metal catalyzed chemical synthesis of unsubstituted polythiophene was reported by Yamamoto et al. in 1980 [58]. In their research work they synthesized polythiophene by reacting 2,5-dibromo-thiophene with Magnesium in the presence of Ni(bipy)Cl₂ catalyst. Magnesium reacts with 2,5-dibromo-thiophene and forms 2-bromo-5-magnesiathiophene. 2-bromo-5-magnesiathiophene couples with Ni and forms dimer which further propagates and forms low molecular weight polythiophene. Lin et al. synthesized polythiophene by treating metal acetylacetonate with Grignard reagent prepared from 2,5-dibromothiophene and magnesium(1:1) in Tetrahydrofuran media [59].

Yoshino et al. reported in their research work that unsubstituted thiophene can be polymerized by FeCl_3 in the presence of chloroform [60]. Fe^{+3} catalyzed oxidative polymerization of thiophene in aqueous media was first reported by Kim et al [61]. They first dispersed thiophene monomer in aqueous media by surfactant SDS which resulted formation of thiophene micelles. These micelles were then transformed into polythiophene by oxidizing thiophene through Fe^{+3} catalysts. Fe^{+3} ions were regenerated by using Hydrogen Peroxide (H_2O_2) which enables to use less amount of catalyst.

3.2.2 ELECTROCHEMICAL SYNTHESIS

Electrochemical synthesis involves use of electrical energy to convert thiophene monomer in to polythiophene. In this method polythiophene is obtained in the form of polythiophene thinfilm on anode in an electrochemical cell. A suitable electrolyte is used to maintain the conductivity of solution. Length of polymer and thickness of polymer film can be adjusted by using different electrode material, current density, voltage, electrolyte, solvent and side chain of thiophene monomer.

3.3 ELECTROPHORETIC DEPOSITION

Electrophoretic deposition technique is the most effective technique for ceramic coatings and processing and widely been used and gaining more interest in the field of ceramic industry. This technique has advantages of high versatility of material use, cost effective, tailored and simplicity. First study of Electrophoretic deposition was reported by Russian scientist in 1808 where he observed movement of clay particles in water when electric potential is applied. Detail study and experimental work was performed by Hamaker in 1940 [62].

Electrophoretic deposition (EPD) is the deposition of charged particles either negative or positive on respective electrode when suitable DC potential is applied across the electrodes. In this method, particles of desired substance are charged positively or negatively in a solution and homogeneous and stable suspension of these particles is made. Movement of these particles towards electrode is made by applying DC across the electrode. Electrophoretic deposition differs from electrolytic deposition as the former involves deposition of charged particles without any redox reaction while the later is deposition of ions by redox reaction [63]. Below is the table that shows the difference between the two.

Table 3.1 Difference between Electrophoretic and Electrolytic Deposition [63]

Property	Electroplating	Electrophoretic deposition
Moving species	Ions	Solid particles
Charge transfer on deposition	Ion reduction	None
Required conductance of liquid medium	High	Low
Preferred liquid	Water	Organic

On the base of deposition of positively charged or negatively charged particles they are classified as cathodic and anodic EPD respectively. Other classification is based on type of solvent viz aqueous and non-aqueous EPD.

Mechanism of EPD explained by Bouyer and Foissy[64, 65] proposed that it is a two step mechanism. First step is migration and depends on bulk properties of the suspended particles i.e. viscosity, conductivity, concentration, size distribution and surface charge density. Next step is deposition of particles on electrode that needs particles to lose their charge when reached at electrode.

Factors that influence the EPD are[64, 65]:

- (i) ***Parameters related to suspended particles***; particle size, dielectric constant of liquid, conductivity, viscosity, zeta potential, stability of suspension,
- (ii) ***Physical parameters***; deposition time, applied voltage, conductivity of substrate,

These controlling parameters can be adjusted to get films of any thickness for almost any material.

3.4 CHARACTERIZATION TECHNIQUES

3.4.1 FTIR SPECTROSCOPY

IR spectroscopy is a qualitative analysis technique where both determination and verification of structure of a compound is carried out. IR spectroscopy utilizes a frequency range from 4000 to 400 cm^{-1} . Bonds in a molecule are in a constant state of vibration. It is the intrinsic property of molecules that they absorb electromagnetic radiations in infrared region when the frequency of infrared radiation matches the natural frequency of vibration of a bond. Thus every peak in an IR

spectrum is result of absorption of IR radiation by specific bond in a molecule. IR spectrum is graph of absorption intensity versus frequency [66].

Each bond in a molecule vibrates with different natural frequency. As same bond in two different molecules exhibits different surrounding environment thus absorbs different frequency radiations. So every molecule has different infrared absorption spectrum. Absorption spectrum can act as finger print for determination of a molecule. By comparing spectrum of a sample with the known spectrum, if they resembles peak by peak, then both substances are thought to be identical.

Fourier transform infrared spectroscopy (FTIR) works on the principle that time-domain spectrum is converted into frequency-domain by using mathematical operation that is fourier-transform. Advantage of FTIR is that analysis of a sample can be performed in less than second.

Infrared spectrophotometer is an instrument that is used to determine the absorption spectrum of a sample. There are two types of infrared spectrophotometers are being used: Fourier transform and dispersive instrument. FT-spectrometer works faster than dispersive spectrometer [66]. A typical FT-spectrometer and schematic diagram is shown below in figure 3.1.



Fig. 3.1a FT-spectrometer

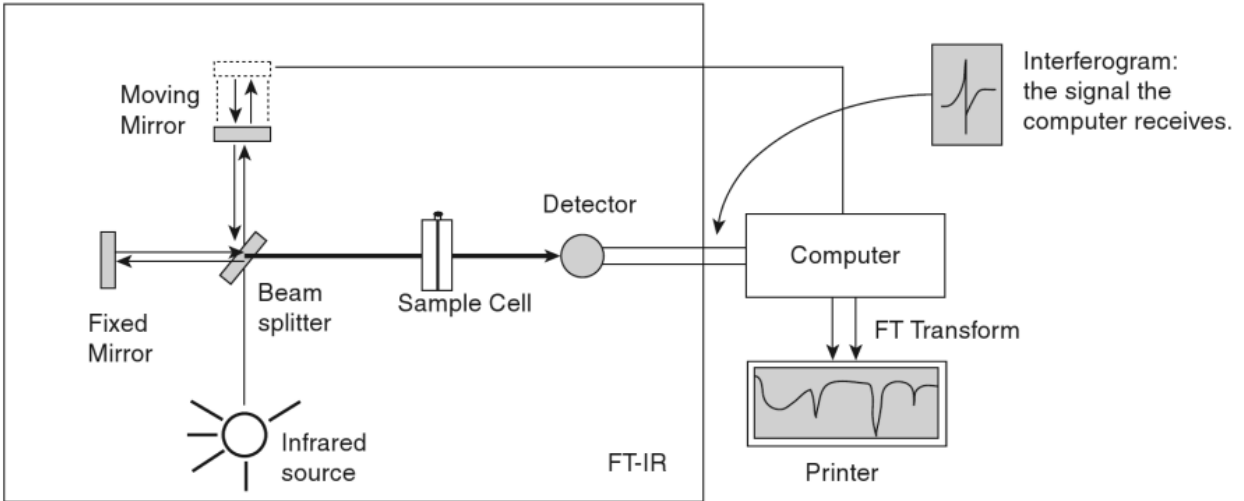


Fig. 3.1b Schematic diagram of Fourier Transform Infrared spectrophotometer[66].

3.4.2 X-RAY DIFFRACTION (XRD)

X-ray diffraction technique is a non-destructive technique employed for both qualitative and quantitative analysis as well as for structural studies of crystalline substances. It is the most valuable technique based on diffraction pattern of material where a small amount of sample is needed to get identification and structural information.

X-ray diffraction works on the principle that when monochromatic x-ray light interacts with the planes of crystalline substance, scattering of x-rays from these planes undergo constructive and destructive interference. This phenomenon is called diffraction. Diffraction through crystalline substances is described by Bragg's Law:

$$2d \sin \theta = n\lambda \quad (\text{Equation 3.1})$$

Where

λ = wavelength of incident light

θ = angle of incidence

d = interplanar distance

n = order of diffraction

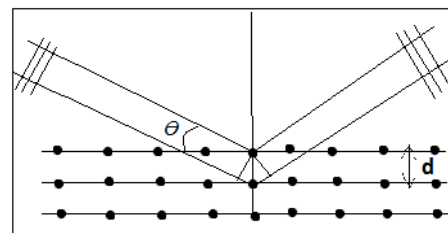


Fig. 3.2 Diffraction through crystal lattice

Diffraction direction depends on the type of unit cell of a crystalline substance while intensity of diffracted rays depends on the orientation of atoms in a crystalline substance. For polycrystalline material, when x-ray beam is subjected, it will scattered through all possible interatomic planes. By changing the detectors angle, all diffraction peaks from the material can be detected[67, 68].

Instrument to measure x-ray diffraction is called diffractometer. On the basis of type of sample it is classified as single crystal diffractometer and powder diffractometer. Generally a diffractometer consist of a source of radiation, monochromator, sample on a turntable, a slit, and detector. A beam of x-rays first passes through monochromator where single wavelength light is chosen and then it strikes the sample. After diffraction from sample the scattered light is detected by detector. Schematic diagram of a typical diffractometer is shown below[67, 68].

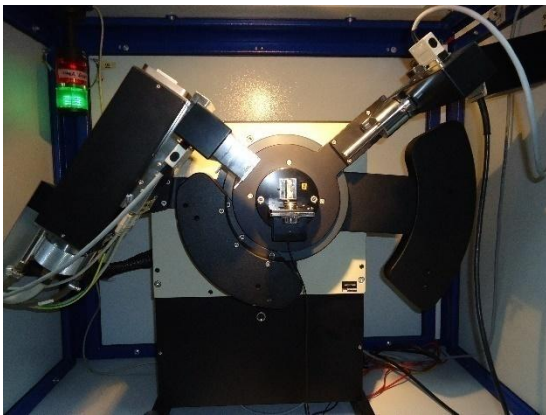
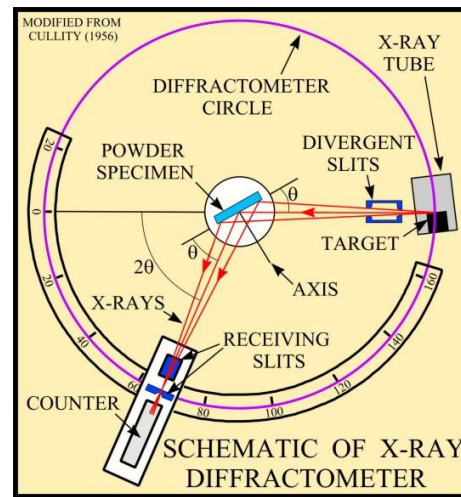


Fig. 3.3 (a) X-Ray Diffractometer STOE θ - θ ,



(b) Schematic diagram of Diffractometer

X-ray diffraction analysis of Barium Titanate, polythiophene and composite was performed by STOE diffractometer. Scan from 2θ value of 5° to 80° was carried out at the scan rate of 0.04 for above samples.

3.4.3 SCANNING ELECTRON MICROSCOPE (SEM)

Scanning electron microscopy utilizes beam of high energy electrons. When high energy electrons interacts with the surface of solid sample, the signals received give information regarding surface morphology of the sample, crystalline structure, shape geometry and particle size of materials. Signals received from the surface of a sample when high energy electron is rastered over the surface is interpreted by generating two dimensional images. Area of 1 cm to 5 microns can be analyzed through SEM. Image of a sample can be magnified up to 300,000 with resolution range of 50 to 100nm[69, 70].

Interaction of electrons with sample generates three types of signals viz secondary electrons (generates SEM images), back scattered electrons and photons which are characteristic x-rays used for elemental analysis (EDS)[69, 70].

A typical Electron Microscope consists of electron gun, magnetic lenses, sample stage, secondary electron detector. Schematic diagram of SEM is illustrated below.

JEOL Scanning Electron Microscope (model JSM 6490LA) was used to take SEM images of Barium Titanate, Polythiophene and composite. SEM images at different magnification and resolution were taken at different operating voltage 10 to 20 kV..

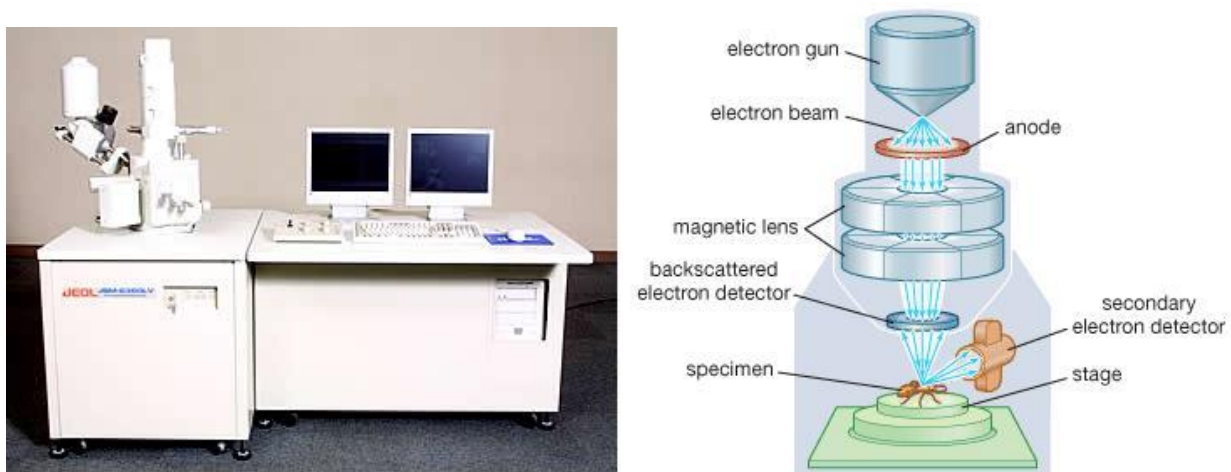


Fig. 3.4. (a) Scanning Electron Microscope (JSM 6490LA), (b) SEM Schematic.

3.4.4 ATOMIC FORCE MICROSCOPE (AFM)

Atomic force microscope is a type of probe microscope where interaction between nano size tip mounted on a cantilever and sample surface gives the information regarding surface topography in the form of image. Images generated through AFM gives details up to atomic level. Tip mounted on cantilever when brought near the surface of sample, it repels or attracts the tip and deflection of cantilever occurs. This deflection is measured by a laser beam reflected from the surface of cantilever on to the photodiode. A feedback mechanism is applied to maintain the constant force between the tip and surface by adjusting the distance between sample and tip. Adjustment of distance is carried through piezoelectric stage by feedback mechanism that moves the tip or sample in x,y and z directions. Signals obtained from movement of cantilever through photodiode are color mapped into an image. An AFM can be operated in both contact and non-contact mode[71, 72].

A typical Atomic Force Microscope consists of a cantilever, nanosize tip, detector, xyz piezoelectric drive, controllers and plotter[72]. Below is shown a schematic diagram of AFM.



Fig. 3.5. (a)AFM JEOL (JSPM-5200), **(b)** Schematic diagram of AFM

Surface topography of thin film of composite prepared through EPD technique was carried out through AFM (JSPM-5200) in tapping mode.

3.4.5 LCR METER

In an LCR meter, press pellet of sample of known thickness is placed in a copper holder. A source of DC applies the direct current through press pellet and current changes with voltage is plotted in a graph. Through these values, dielectric properties of material can be calculated.

Dielectric properties of pressed pellets of composites at room temperature and ambient atmosphere were studied by Waynekerr impedance analyzer 6505 an LCR meter shown below.

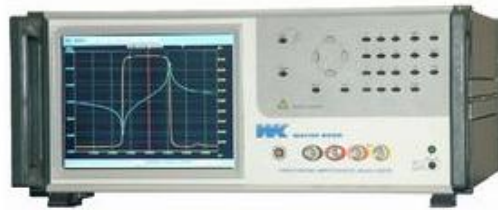


Fig.3.6 Waynekerr impedance analyzer 6505

4 EXPERIMENTAL WORK

4.1 BARIUM TITANATE SYNTHESIS

Ba(OH)₂.8H₂O (Merck) as Barium precursor and TiO₂ (Scharlau Spain) as Titanium precursor are used for Hydrothermal synthesis of Barium Titanate (BaTiO₃). Both Ba(OH)₂.8H₂O and TiO₂ are used in 1:1 ratio as BaTiO₃ formation consumes equimolar ratio. Both precursors dissolved in 60ml of DD water are kept in Teflon vessels. The pH adjustment is not required as concentration of Ba(OH)₂ in solution is sufficient to reach the alkalinity (pH: 9-10) necessary to precipitate out BaTiO₃. Reaction is performed in an autoclave at 120°C for 24 hrs [73]. The obtained slurry was washed with 1 M formic acid and distilled water to remove BaCO₃. Washed slurry was dried at 120 °C in a furnace for 24 hr. The resulted product was grinded to get BaTiO₃ powder.

4.2 PTH/ BaTiO₃ COMPOSITE SYNTHESIS

The PTh/BaTiO₃ hybrid composite was synthesized by in situ heterogeneous Cu(II) catalyzed oxidative polymerization of thiophene[6] in presence of Barium Titanate nanoparticles. First BaTiO₃ nanoparticles were functionalized with SDS and then dispersed in 60ml of DD water through sonication. After that thiophene monomer was added to BaTiO₃ dispersion and sonicated for 1h to adsorb monomer on the surface of BaTiO₃. Temperature was raised up to 50°C. Then 9g of 30% H₂O₂ solution (Scharlau Spain) and 0.2mmol Cu(II) sulphate pentahydrate dissolved in 5ml water were added in one portion. A color change from white to off white was observed which indicated the formation of polymer. The reaction was allowed to proceed for 7h. After 7h, off white precipitates were obtained. The product was washed with water and ethanol alternatively to remove Cu (II) salt and unreacted thiophene. After that it was dried for 24h at 50°C under vacuum condition in a vacuum oven. Different fractions of BaTiO₃ nanoparticles in BaTiO₃-PTh composites were employed.

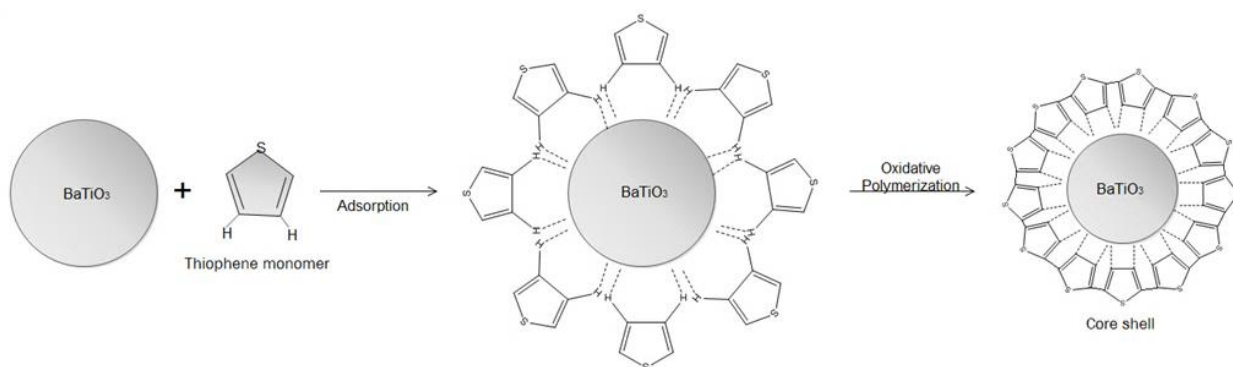


Fig. 4.1 Schematic drawing of core shell formation process.

4.3 ELECTROPHORETIC THINFILM DEPOSITION OF PTH/BATiO₃

4.3.1 SUBSTRATES USED FOR ELECTROPHORETIC DEPOSITION

For electrophoretic deposition of Composite, it is necessary that substrate must be conductive. Therefore two types of substrates were used:

- First one was ITO on Glass
- And Second one polished Cu strips

4.3.2 CLEANING OF SUBSTRATE

Substrates were cleaned from dust and organic matters to get smooth and well adhered thinfilm. For this purpose, it was soaked in acetone and sonicated for 30min. After that it was dried with dry and hot air.

4.3.3 SOLVENTS USED FOR SUSPENSION PREPARATION

Numerous solvents and combinations were used to get a better suspension of composite. Different solvents tested are as follows:

- Water
- Ethanol
- Propanol
- Acetone
- THF
- Ethanol-Propanol Mix(1:1)

About 0.05g of composite material was dispersed in 50ml of above mentioned solvents. 2ml of 0.1M acetic acid was added to get the pH of 3.5. Dispersion was homogenized by sonication for 1 hour. The suspension was allowed to stand for 1 day before use. The suspension was quite stable after 24hr.



Fig. 4.2 Suspension of composite in Propanol-Water Mixture

4.3.4 ELECTROPHORETIC DEPOSITION OF THINFILM

The process was carried out in a beaker with two electrodes; platinum anode and a cathode (ITO, Cu) using DC power source (0.1-60V). Multimeter (Kiethlay) was used for recording the current. Deposition was performed at room temperature and ambient atmosphere. The dispersion was stirred continuously during the deposition. The Schematic arrangement of EPD cell is shown in figure 4.3.

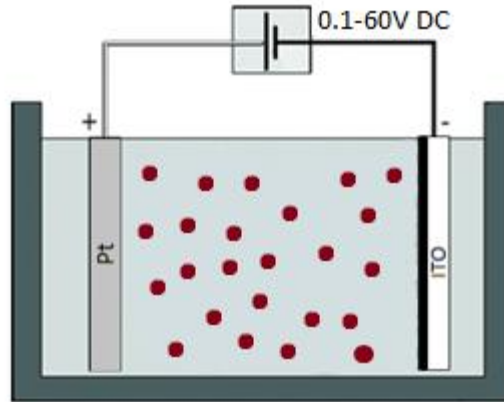


Fig. 4.3 Schematic diagram of cell for Electrophoretic Deposition

4.3.5 VACUUM DRYING

The resulted thinfilm was dried in a vacuum oven at 50°C for 24hr to remove all the moisture.

4.3.6 ANNEALING

Well dried thinfilm on ITO substrate was subjected to annealing. For this purpose it was heated at 200°C in a muffle furnace for 8 hrs at the rate of 2°C min⁻¹.

5 RESULTS AND DISCUSSION

5.1 MORPHOLOGY OF COMPOSITE PARTICLES

Morphology of the composite particles was investigated by SEM. In Fig. 3, SEM micrographs of single composite particle along with composites having different fractions of polythiophene are presented.

In Fig. 5.1a and b, single particle and agglomerates were focused where they clearly shows the successful coating of polythiophene on BaTiO₃ nanoparticles. Electron beam penetrates more in polymer then denser ceramic particles. So here we can infer that denser area is the BaTiO₃ core while outer lighter shell belongs to polythiophene.

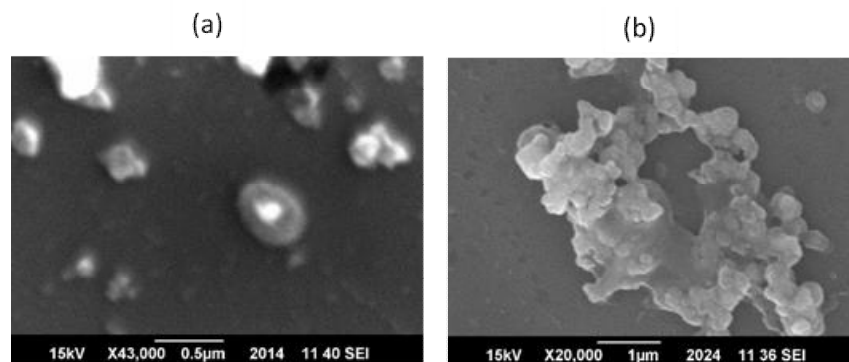


Fig. 5.1 SEM micrographs of BaTiO₃-PTh Nanoparticles.

It can be clearly infer from the micrographs in fig. 5.2 that by increasing the percentage of polythiophene from 10% to 40%, particle nature of composite is gradually replaced by cluster type and submicron size particles. For 10% polythiophene, BT particles are more distinct while at 40% percent BaTiO₃ particles cannot be distinguished rather they are embedded in polythiophene matrix. Composite with 40% polythiophene also contain some tetragonal micro size polythiophene particles with embedded BT.

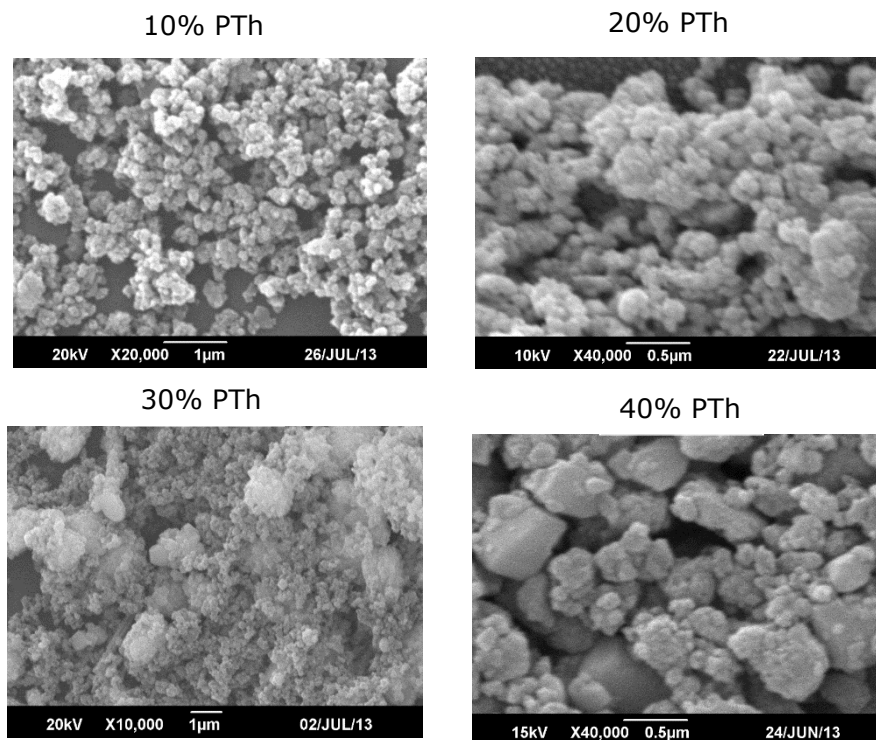


Fig. 5.2 SEM micrographs of BaTiO₃-PTh Nanocomposite.

5.2 CHEMICAL STRUCTURE OF COMPOSITE

5.2.1 FOURIER TRANSFORM INFRARED SPECTROSCOPY (FTIR)

Fig. 5.3 shows the FTIR spectra of BaTiO₃, PTh and BaTiO₃-PTh nanocomposite. Two distinct peaks at 560 and 440 cm⁻¹ are the characteristic peaks of BT in BaTiO₃ spectrum. Bands at 3418cm⁻¹ and 2932cm⁻¹ in PTh are originated from O-H stretching vibration of water in KBr. Peak at 2854cm⁻¹ represents C-H asymmetric stretching of polythiophene[74]. The peaks at 1628 and 1385cm⁻¹ corresponds to C=C symmetric and asymmetric stretching in PTh spectrum[75]. In BaTiO₃-PTh spectrum, the stretching frequencies of C_β-H at about 1035 and 788 cm⁻¹ in the reported polythiophene spectrum [76] were shifted to 1077 and 983 cm⁻¹ respectively due to the formation of hydrogen bond between Polythiophene and BaTiO₃. While band at 1123 cm⁻¹ belongs to C_α- C_α resonance absorption between two thiophene rings[76]. Sharp peak at 610cm⁻¹ was assigned to C-S-C ring deformation. All peaks in Polythiophene and composite matches except little change in intensity at 1000 to 1200 cm⁻¹. From above analysis we can infer that BaTiO₃-PThnanocomposite has successfully been prepared.

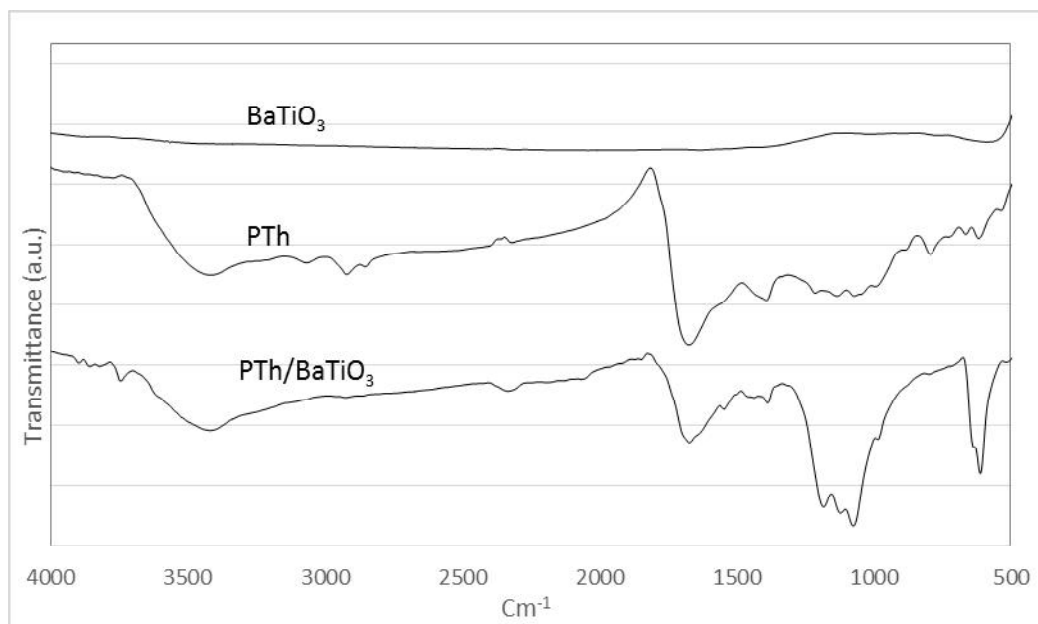


Fig. 5.3 FTIR spectrum of Barium Titanate(BT), Polythiophene(PTh) and PTh/BT Composite(BTPTH)

5.2.2 X-RAY DIFFRACTION (XRD)

X-ray diffraction patterns of both pure PTh and BaTiO₃-PTh composite are represented in Figure 5. Pure polythiophene(PTh) which is amorphous in nature, shows a wide amorphous peak at around 23° as shown in curve. It corresponds to intermolecular π - π stacking structure and amorphous packing of polymer[40]. BaTiO₃-PTh composite XRD pattern shows characteristic BaTiO₃ peaks (■) but the intensity of the main peaks characterizing BT becomes weakened as well as some extra peaks were also observed. This change in intensity is due to the influence of amorphous PTh on the crystallinity of BT particles.

Thus both FTIR and XRD results clearly indicate the formation of Polythiophene/BaTiO₃ nanocomposite without any change in the chemical structure of both components.

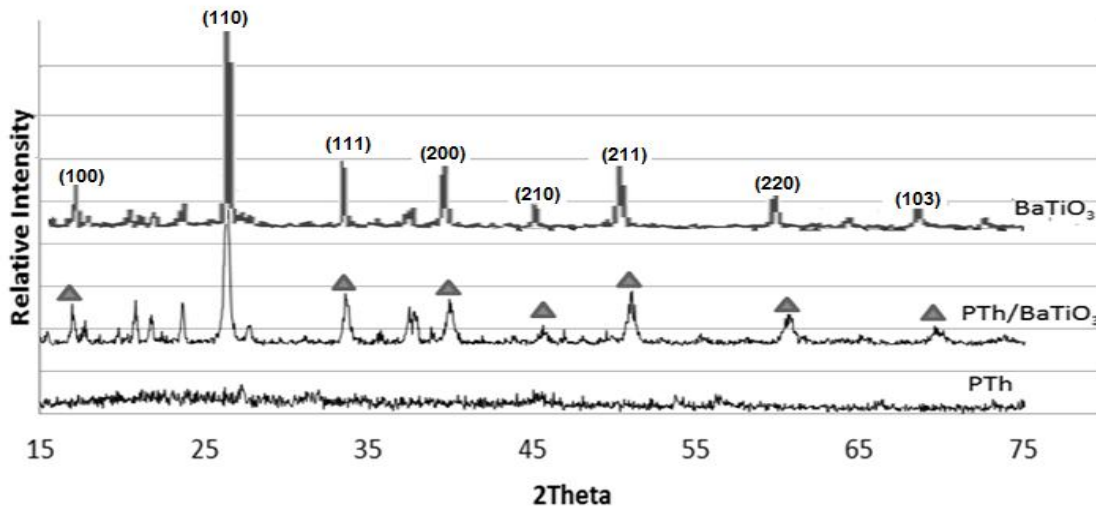


Fig. 5.4 XRD patterns of BariumTitanate($BaTiO_3$), Polythiophene(PTh) and PTh/ $BaTiO_3$ nanoparticles

5.3 ELECTROPHORETIC DEPOSITION

Thin films of composite were electrophoretically deposited on conducting substrate by using it as electrode. Using conducting substrate was not an issue as dielectric materials used in capacitor must be employed in the form of layer between two conductive plates. Therefore, substrate can be used as one plate of capacitor. Both ITO and Copper were found to have good affinity to composite particles in solution. Therefore film formed was intact firmly to the substrate. Particles to deposit electrophoretically must be dispersed and have good stability in solvent. Coating of polymer made the BT particles to disperse easily in the mixture of water and propanol by providing stearic stability. Also addition of HCl charged the particles positively. When potential of 3V was applied, positively charged particles were migrated to cathode. The electrophoretic deposition technique was used to prepare thin film on conducting substrate. About 0.05g composite was added in to the solution of 40ml of propanol and water in equal proportion. Acetic acid was added in an amount to make 0.1M out of above solution for surface charging of the particles. The dispersion was sonicated for 1 hour to make a homogenous stable dispersion. A potential of 10V was applied across the two electrodes at room temperature and in

ambient atmosphere. During deposition stirring was performed to make homogenous film. Fig. 7 shows the schematic drawing of process and mechanism.

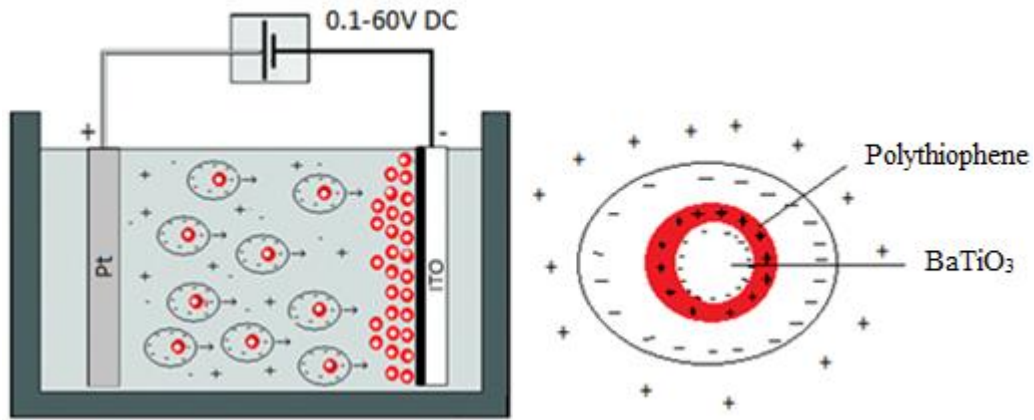


Fig. 5.5 Schematic drawing of process and mechanism of EPD

The thin films thus prepared were characterized by SEM and AFM. Uniform films with average roughness of 9nm and thickness of 244.5nm of composite were prepared. Below in Fig. 5.6 and 5.7 is shown the SEM and AFM micrographs of thin film electrophoretically deposited.

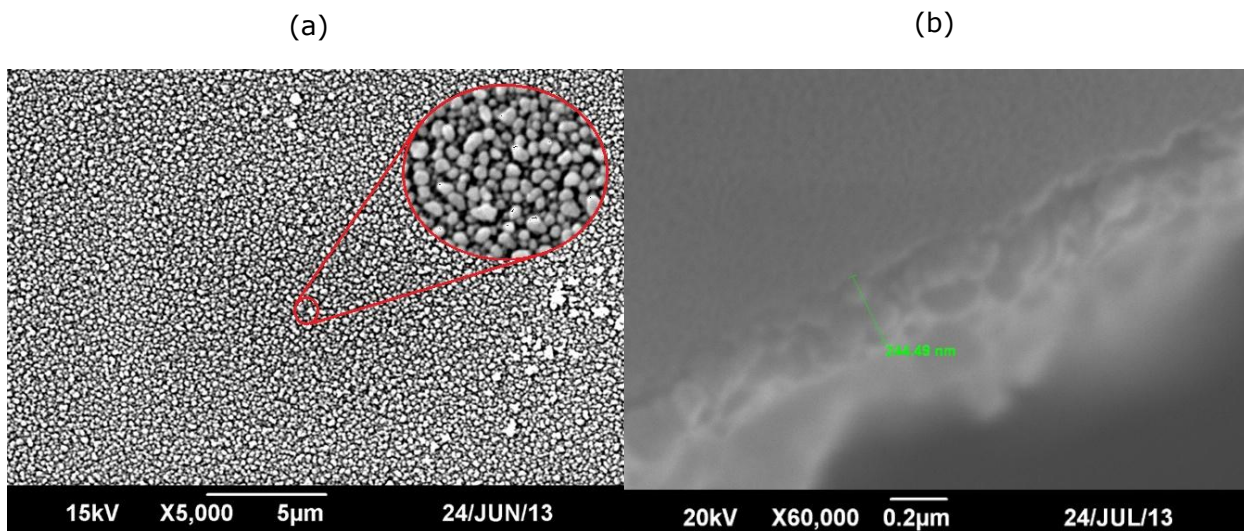


Fig. 5.6 SEM micrographs of thin films: (a) Surface Morphology, (b) Film thickness.

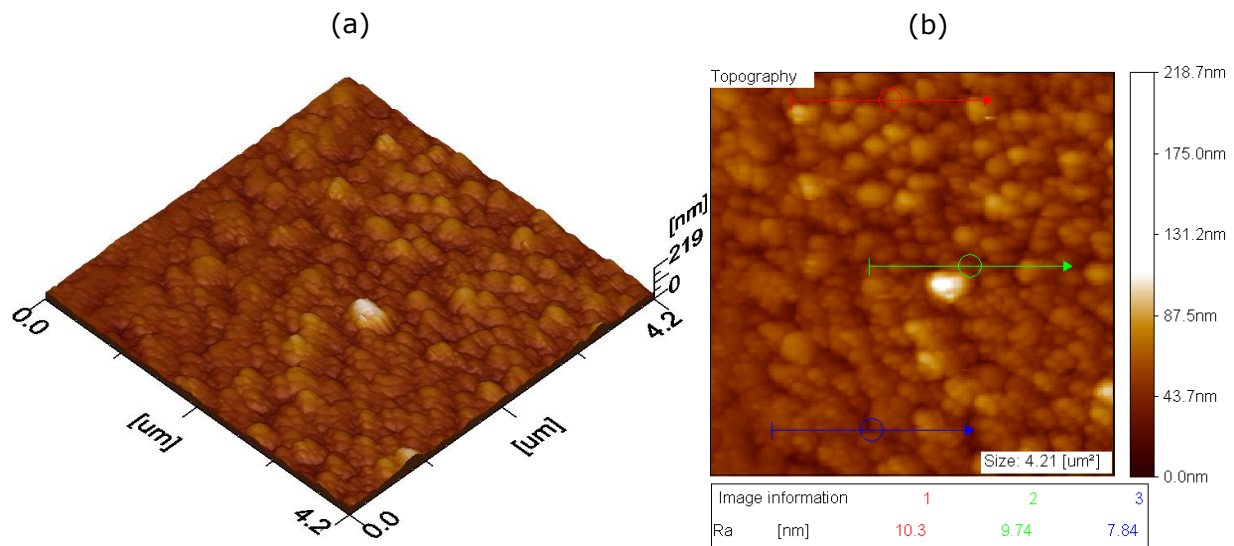


Fig. 5.7 AFM images of thin film: (a) 3D surface topography, (b) surface roughness.

5.4 DIELECTRIC MEASUREMENTS

The dielectric permittivity was calculated using relation 1. The variations of frequency dependent complex dielectric permittivity with addition of Polythiophene % in BaTiO₃ have been shown in Figure 5.8. It can be seen from the figure that real parts of complex permittivity decreased from 47 to 14 with increase in Polythiophene % for all the samples at room temperature in low frequency region. The dielectric permittivity decreased as the applied frequency is increased from 100 Hz to 5 MHz. The decrease of dielectric permittivity with frequency is due to the decrease of the orientation polarization, since it takes longer time than other types of polarization and the dipoles cannot be able to rotate rapidly, so that their oscillations lag behind the field. As the applied frequency is further increased the dipole will be completely unable to follow the alternating field and the orientation polarization stopped; so dielectric permittivity decreases approaching a constant value at high frequencies due to the space charge polarization. The space charges are able to follow the frequency of an applied field at low frequency while they may not undergo relaxation at high frequencies.

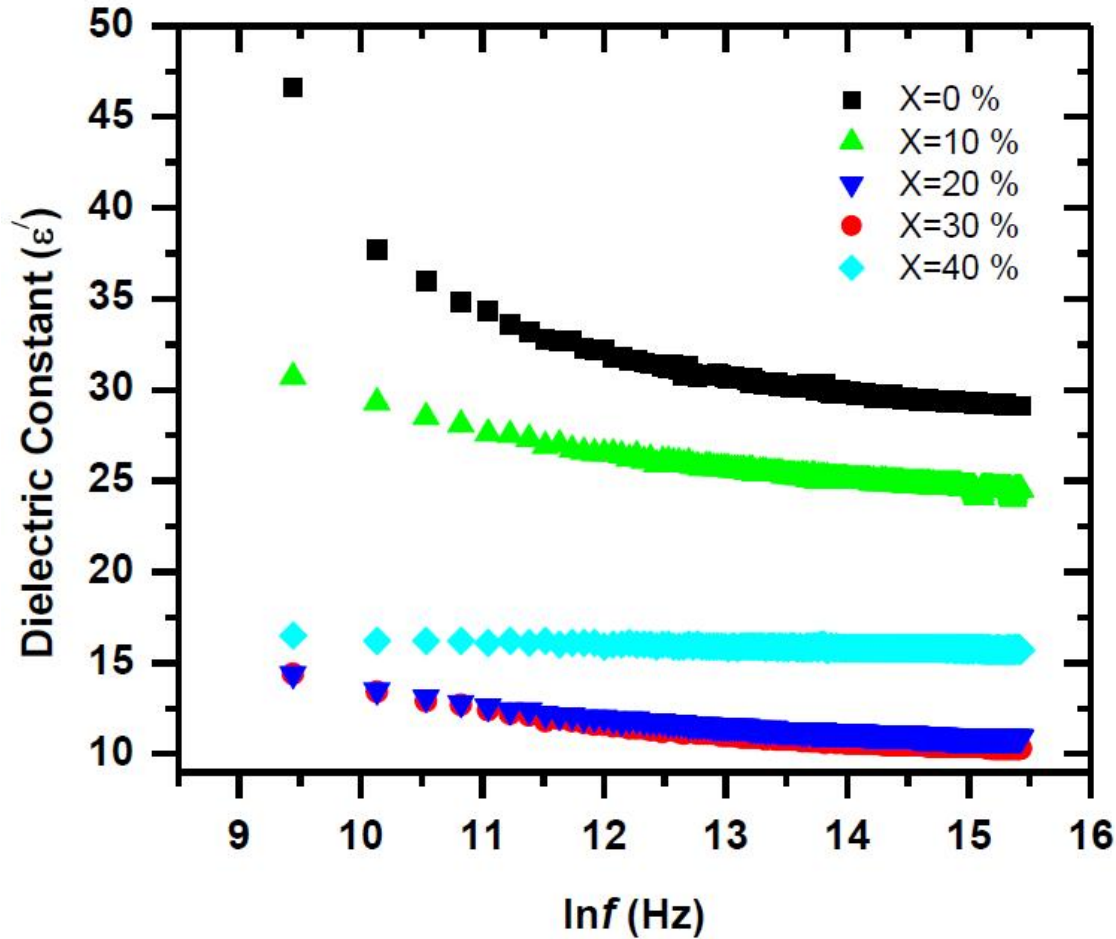


Fig. 5.8 Comparison of Dielectric constant of press pellets (X=%age of polythiophene)

The dielectric loss tangent ($\tan\delta$) was measured using relation 2. The dielectric loss tangent represents the energy loss within the dielectric medium. The frequency dependence of the dielectric loss tangent with addition of Polythiophene % in BaTiO₃ system at room temperature is shown in Figure 5.9. The values of dielectric loss tangent at low frequency decreased from 0.55 to 0.045 as the concentration of Polythiophene increased from 0% to 40%. It can be seen from figure 10 the dielectric loss tangent is observed to decrease rapidly in the low frequency region; the rate of decrease slows down as the frequency rises and finally becomes almost constant at high frequencies. This behavior of BaTiO₃ with addition of Polythiophene % can be explained on the basis that in the low frequency region, which corresponds to the high resistivity of grain boundaries, more energy is required for electron hopping and as a result the loss is high.

In the high frequency region, which corresponds to the high conductivity of grain, energy required for the hopping of electrons is less and dielectric loss tangent decreases [26,27].

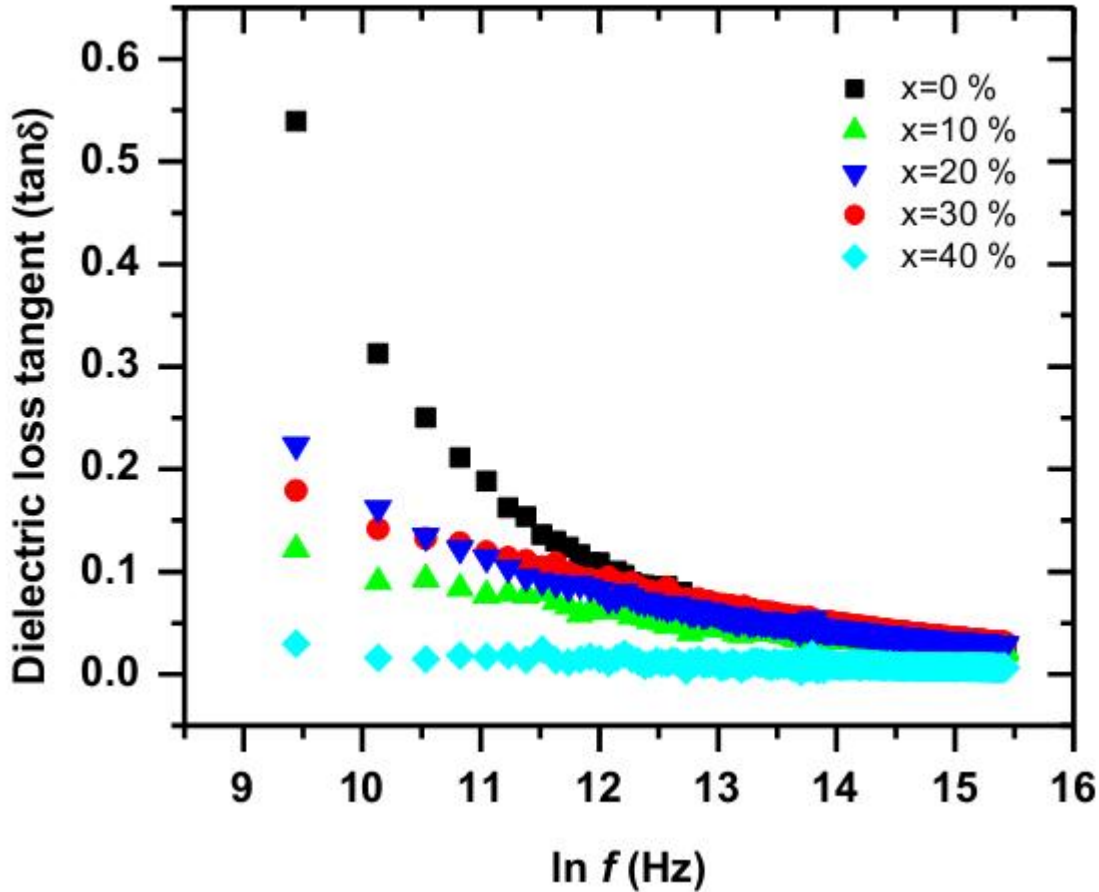


Fig. 5.9 Comparison of Dielectric loss tangent ($\tan\delta$) of press pellets ($X = \%$ age of polythiophene).

The dielectric loss (ϵ'') was determined using equation 3. Dielectric loss is an important part of the total core loss in materials. The dielectric loss decreased from 25 to 0.1 as the concentration of BaTiO₃ with Polythiophene % increases. Hence for low core loss, low dielectric losses are desirable. The dielectric loss as a function of frequency for all the compositions is shown in figure 5.10. The dielectric loss profiles are similar to those of the real part of dielectric constant. The increase in hopping electrons result in a local displacement in the direction of the extent electric field causing an increase in electric polarization enhances dielectric loss.

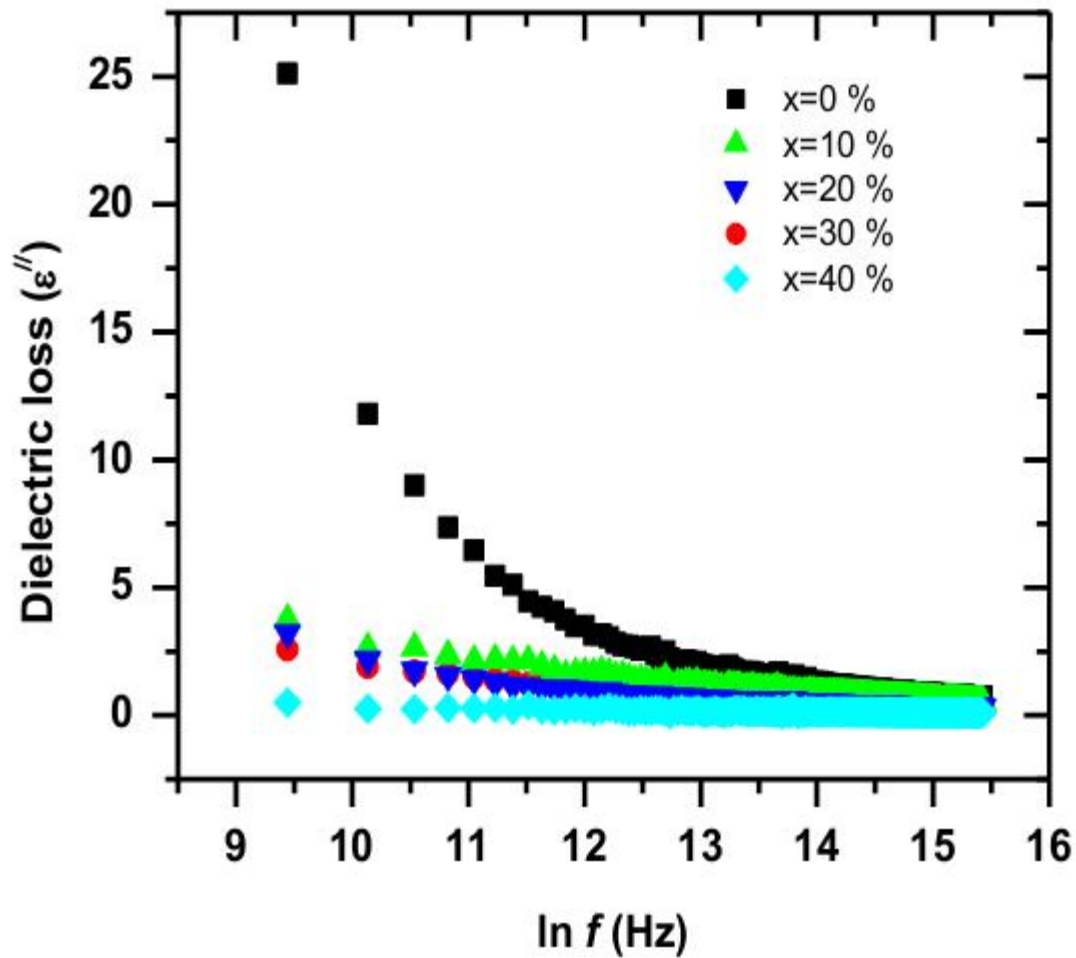


Fig. 5.10 Comparison of Dielectric loss (ϵ'') of press pellets ($X = \%$ age of polythiophene)

AC conductivity is calculated using relation 4. The variation of AC conductivity as a function of frequency and composition at room temperature has been shown in Figure 5.11. It is obvious from the graphs that AC conductivity increases linearly with frequency of the applied field and decreases with increasing the concentration of Polythiophene % in BaTiO_3 with. At lower frequencies grain boundaries influence on conduction is more as compared to grain which contributes more in high frequencies. It can be observed also that AC conductivity decreases with increase of Polythiophene % concentration in the BaTiO_3 . The reason for such decrease in conductivity can be explained by microstructure and the jumping probability and jump length.

Smaller the grain size greater will be the insulating grain boundaries and less will be the conductivity of the material.

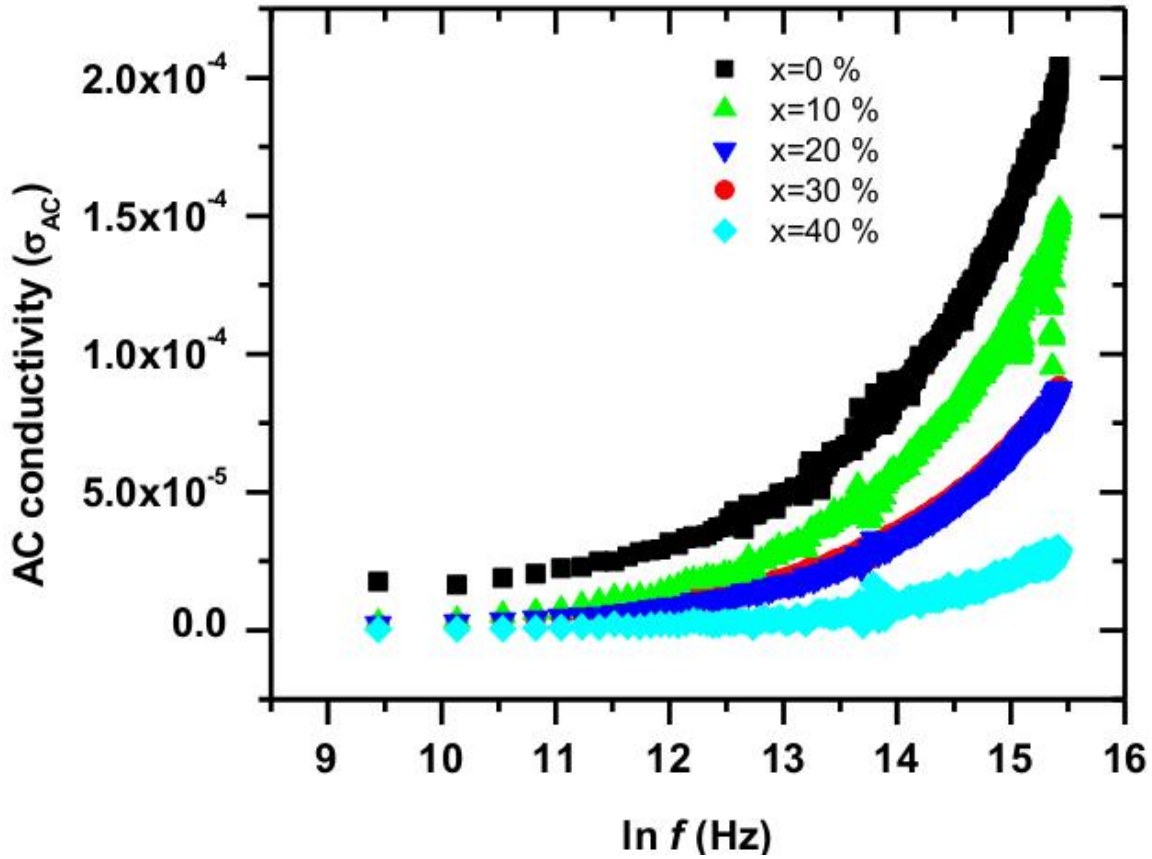


Fig. 11 Comparison of AC conductivity (σ_{AC}) of press pellets (X = %age of polythiophene).

The dielectric constant was determined from the formula

$$\epsilon' = \frac{Cd}{\epsilon_0 A} \quad \text{(Equation 5.1)}$$

Where C is the capacitance of the pellet in farad, d the thickness of the pellet in meter, A the cross-sectional area of the flat surface of the pellet and ϵ_0 the constant of permittivity of free space.

The dielectric tangent loss factor can be calculated using the relation

$$\tan\delta = \frac{1}{2\pi f R_p C_p} \quad (\text{Equation 5.2})$$

Where δ is the loss angle, f is the frequency, R_p is the equivalent parallel resistance and C_p is the equivalent parallel capacitance.

The dielectric loss (ϵ'') is also measured in terms of tangent loss factor ($\tan\delta$) defined by the relation:

$$\epsilon'' = \epsilon' \tan\delta \quad (\text{Equation 5.3})$$

The AC conductivity can be calculated using the values of frequency and dielectric loss factors.

$$\sigma_{AC} = 2\pi f \epsilon_0 \epsilon' \tan\delta \quad (\text{Equation 5.4})$$

Where ϵ_0 , ϵ' and $\tan\delta$ are defined above.

6 CONCLUSION

The PTh/BaTiO₃ Nano composites consist of nanoparticles with BaTiO₃ core and PTh shell were prepared by the oxidative polymerization of thiophene in the presence of BT particles in dispersed form. XRD and FTIR confirmed that both polythiophene and BT did not lose their chemical identity. By means of scanning electron microscopy, the expected core-shell structure of the BT/PTh nano composite was confirmed. Dielectric properties of pressed pellets of composite with different BT-PTh ratio were investigated by LCR meter. It was observed that by increasing the percentage of PTh while keeping the other variables constant, a decrease in dielectric constant as well as dielectric loss occurs. The Electrophoretic deposition technique was used for the preparation of smooth and thin film with average thickness of 260nm and roughness of 8nm out of composite on conducting substrates (Cu,ITO,SS). Various conditions such as concentration, time and voltage can be employed to prepare films of different thickness and particle size. Such films can further be characterized for capacitance behavior and can have wide applications in capacitors and FETs [77].

REFERENCES

- [1] H. S. Nalwa, *Handbook of Low and High Dielectric Constant Materials and Their Applications, Two-Volume Set*: Academic Press, 1999.
- [2] P. Barber, S. Balasubramanian, Y. Anguchamy, S. Gong, A. Wibowo, H. Gao, *et al.*, "Polymer composite and nanocomposite dielectric materials for pulse power energy storage," *Materials*, vol. 2, pp. 1697-1733, 2009.
- [3] Z. M. Dang, Y. Q. Lin, H. P. Xu, C. Y. Shi, S. T. Li, and J. Bai, "Fabrication and dielectric characterization of advanced BaTiO₃/polyimide nanocomposite films with high thermal stability," *Advanced Functional Materials*, vol. 18, pp. 1509-1517, 2008.
- [4] H. C. Pant, M. K. Patra, A. Verma, S. R. Vadera, and N. Kumar, "Study of the dielectric properties of Barium Titanate-polymer composites," *Acta materialia*, vol. 54, pp. 3163-3169, 2006.
- [5] S. Liang, S. R. Chong, and E. P. Giannelis, "Barium Titanate/epoxy composite dielectric materials for integrated thin film capacitors," in *Electronic Components & Technology Conference, 1998. 48th IEEE*, 1998, pp. 171-175.
- [6] Z. Wang, Y. Wang, D. Xu, E. S. W. Kong, and Y. Zhang, "Facile synthesis of dispersible spherical polythiophene nanoparticles by copper (II) catalyzed oxidative polymerization in aqueous medium," *Synthetic Metals*, vol. 160, pp. 921-926, 2010.
- [7] K. Kinoshita and A. Yamaji, "Grain size effects on dielectric properties in barium Titanate ceramics," *Journal of Applied Physics*, vol. 47, pp. 371-373, 1976.
- [8] A. R. Von Hippel, *Dielectric materials and applications*: Artech House, 1954.
- [9] E. Murphy and S. Morgan, "The Dielectric Properties of Insulating Materials," *Bell System Technical Journal*, vol. 17, pp. 640-669, 1938.
- [10] X. Hao, "A review on the dielectric materials for high energy-storage application," *Journal of Advanced Dielectrics*, vol. 3, 2013.
- [11] B. Vul and I. Goldman, "Dielectric constant of barium Titanate as a function of strength of an alternating field," *Compt. Rend. Acad. Sci. URSS*, vol. 49, pp. 177-80, 1945.
- [12] B. Wul and I. Goldman, "Dielectric hysteresis in barium Titanate," *Comptes Rendus URSS*, vol. 46, p. 139, 1945.
- [13] F. Jona and G. Shirane, *Ferroelectric crystals* vol. 1: Pergamon, 1962.
- [14] R. C. Buchanan, *Ceramic materials for electronics* vol. 25: CRC press, 2004.
- [15] F. Moura Filho, "Comportamento dielétrico e ferroelétrico de cerâmicas BA ('TI IND1-X'ZR IND. X)'O IND. 3'modificadas com íons vanádio e tungstênio obtidos a partir de mistura de óxidos," 2008.
- [16] www.3dchem.com/inorganicmolecule.asp?id=1618 [Online].
- [17] Z. Lazarevica, N. Romcevica, M. Vijatovicb, N. Paunovica, M. Romcevica, B. Stojanovicb, *et al.*, "Characterization of barium Titanate ceramic powders by Raman spectroscopy," in *Proceedings of the Tenth Annual Conference of the Materials Research Society of Serbia*, 2008.
- [18] M. Cernea, "Sol-gel synthesis and characterization of BaTiO₃ powder," *Journal of Optoelectronics and Advanced Materials*, vol. 7, p. 3015, 2005.
- [19] M. Boulos, S. Guillemet-Fritsch, F. Mathieu, B. Durand, T. Lebey, and V. Bley, "Hydrothermal synthesis of nanosized BaTiO₃ powders and dielectric properties of corresponding ceramics," *Solid State Ionics*, vol. 176, pp. 1301-1309, 2005.
- [20] A. Testinon, M. T. Buscaglia, M. Viviani, V. Buscaglia, and P. Nanni, "Synthesis of BaTiO₃ particles with tailored size by precipitation from aqueous solutions," *Journal of the American Ceramic Society*, vol. 87, pp. 79-83, 2004.
- [21] V. Vinothini, P. Singh, and M. Balasubramanian, "Synthesis of barium Titanate nanopowder using polymeric precursor method," *Ceramics international*, vol. 32, pp. 99-103, 2006.
- [22] N. C. M. sharma, "The dielectric properties of pure barium Titanate as a function of grain size," *journal of the Australian ceramic society* vol. 10, pp. 16-20, 1974.

- [23] K. Ishikawa, K. Yoshikawa, and N. Okada, "Size effect on the ferroelectric phase transition in PbTiO₃ ultrafine particles," *Physical Review B*, vol. 37, p. 5852, 1988.
- [24] W. Buessem, L. Cross, and A. Goswami, "Phenomenological Theory of High Permittivity in Fine-Grained Barium Titanate," *Journal of the American Ceramic Society*, vol. 49, pp. 33-36, 1966.
- [25] H. Martirena and J. Burfoot, "Grain-size effects on properties of some ferroelectric ceramics," *Journal of Physics C: Solid State Physics*, vol. 7, p. 3182, 1974.
- [26] G. Arlt and D. Hennings, "Dielectric properties of fine-grained barium Titanate ceramics," *Journal of applied physics*, vol. 58, pp. 1619-1625, 1985.
- [27] Y. Kobayashi, A. Nishikata, T. Tanase, and M. Konno, "Size effect on crystal structures of barium Titanate nanoparticles prepared by a sol-gel method," *Journal of sol-gel science and technology*, vol. 29, pp. 49-55, 2004.
- [28] I. Bunget and M. Popescu, *Physics of solid dielectrics* vol. 19: Elsevier Science Ltd, 1984.
- [29] J. Kuffel, E. Kuffel, and W. S. Zaengl, *High voltage engineering fundamentals*: Newnes, 2000.
- [30] Y. Sun, Z. Zhang, and C. Wong, "Influence of interphase and moisture on the dielectric spectroscopy of epoxy/silica composites," *Polymer*, vol. 46, pp. 2297-2305, 2005.
- [31] V. Martina, K. Ionescu, L. Pigani, F. Terzi, A. Ulrici, C. Zanardi, *et al.*, "Development of an electronic tongue based on a PEDOT-modified voltammetric sensor," *Analytical and bioanalytical chemistry*, vol. 387, pp. 2101-2110, 2007.
- [32] M. G. Harrison and R. H. Friend, "Optical applications," *Electronic Materials: The Oligomer Approach*, pp. 516-558, 1998.
- [33] F. Garnier, "Field-Effect Transistors Based on Conjugated Materials," *Electronic Materials: The Oligomer Approach*, pp. 559-583, 1998.
- [34] G. Schopf and G. Kößmehl, *Polythiophenes-electrically conductive polymers* vol. 129: Springer Berlin, 1997.
- [35] M. S. Halper and J. C. Ellenbogen, "Supercapacitors: A brief overview," *The MITRE Corporation, McLean, Virginia, USA*, pp. 1-34, 2006.
- [36] S. P. Gnanakan, M. Rajasekhar, and A. Subramania, "Synthesis of polythiophene nanoparticles by surfactant-assisted dilute polymerization method for high performance redox supercapacitors," *Int. J. Electrochem. Sci*, vol. 4, pp. 1289-1301, 2009.
- [37] K. A. Noh, D.-W. Kim, C.-S. Jin, K.-H. Shin, J. H. Kim, and J. M. Ko, "Synthesis and pseudocapacitance of chemically-prepared polypyrrole powder," *Journal of power sources*, vol. 124, pp. 593-595, 2003.
- [38] D. K. Bhat and M. S. Kumar, "N and p doped poly (3, 4-ethylenedioxythiophene) electrode materials for symmetric redox supercapacitors," *Journal of materials science*, vol. 42, pp. 8158-8162, 2007.
- [39] C. Arbizzani, M. Gallazzi, M. Mastragostino, M. Rossi, and F. Soavi, "Capacitance and cycling stability of poly (alkoxythiophene) derivative electrodes," *Electrochemistry communications*, vol. 3, pp. 16-19, 2001.
- [40] B. Senthilkumar, P. Thenamirtham, and R. Kalai Selvan, "Structural and electrochemical properties of polythiophene," *Applied Surface Science*, vol. 257, pp. 9063-9067, 2011.
- [41] T. Lewis, "Interfaces: nanometric dielectrics," *Journal of Physics D: Applied Physics*, vol. 38, p. 202, 2005.
- [42] T. Lewis, "Interfaces are the dominant feature of dielectrics at the nanometric level," *Dielectrics and Electrical Insulation, IEEE Transactions on*, vol. 11, pp. 739-753, 2004.
- [43] T. Tanaka, M. Kozako, N. Fuse, and Y. Ohki, "Proposal of a multi-core model for polymer nanocomposite dielectrics," *Dielectrics and Electrical Insulation, IEEE Transactions on*, vol. 12, pp. 669-681, 2005.
- [44] J. Li, J. Claude, L. E. Norena-Franco, S. I. Seok, and Q. Wang, "Electrical energy storage in ferroelectric polymer nanocomposites containing surface-functionalized BaTiO₃ nanoparticles," *Chemistry of Materials*, vol. 20, pp. 6304-6306, 2008.

- [45] P. Kim, N. M. Doss, J. P. Tillotson, P. J. Hotchkiss, M.-J. Pan, S. R. Marder, *et al.*, "High energy density nanocomposites based on surface-modified BaTiO₃ and a ferroelectric polymer," *ACS nano*, vol. 3, pp. 2581-2592, 2009.
- [46] P. Kim, S. C. Jones, P. J. Hotchkiss, J. N. Haddock, B. Kippelen, S. R. Marder, *et al.*, "Phosphonic acid-modified barium Titanate polymer nanocomposites with high permittivity and dielectric strength," *Advanced Materials*, vol. 19, pp. 1001-1005, 2007.
- [47] S. Liang, S. R. Chong, and E. P. Giannelis, "Barium Titanate/epoxy composite dielectric materials for integrated thin film capacitors," in *Electronic Components & Technology Conference, 1998. 48th IEEE*, 1998, pp. 171-175.
- [48] H. B. Sharma, H. Sarma, and A. Mansingh, "Fatigue in sol-gel derived barium Titanate films," *Journal of applied physics*, vol. 85, pp. 341-346, 1999.
- [49] S. Kim, T. Fujimoto, T. Manabe, I. Yamaguchi, T. Kumagai, and S. Mizuta, "Dense and smooth epitaxial BaTiO₃ thin films by the dipping-pyrolysis process," *Journal of materials research*, vol. 14, pp. 592-596, 1999.
- [50] B. Hoerman, G. Ford, L. Kaufmann, and B. Wessels, "Dielectric properties of epitaxial BaTiO₃ thin films," *Applied physics letters*, vol. 73, pp. 2248-2250, 1998.
- [51] C. Feldman, "Formation of thin films of BaTiO₃ by evaporation," *Review of Scientific Instruments*, vol. 26, pp. 463-466, 1955.
- [52] A. Feuersanger, A. Hagenlocher, and A. Solomon, "Preparation and properties of thin barium Titanate films," *Journal of the Electrochemical Society*, vol. 111, pp. 1387-1391, 1964.
- [53] G. Smolenskii, *Ferroelectrics and related materials* vol. 3: Taylor & Francis US, 1984.
- [54] P. Phule and S. Risbud, "Sol-gel synthesis of barium Titanate powders using barium acetate and titanium (IV) isopropoxide," *Advanced Ceramic Materials;(USA)*, vol. 3, 1988.
- [55] H. Maie, C. U. M. Science, and Engineering, *Synthesis and Dielectric Properties of Nanocrystalline Barium Titanate and Silver/barium Titanate Particles*: Clemson University, 2008.
- [56] W. L. Suchanek and R. E. Riman, "Hydrothermal synthesis of advanced ceramic powders," *Advances in Science and Technology*, vol. 45, pp. 184-193, 2006.
- [57] W. S. Clabaugh, E. M. Swiggard, and R. Gilchrist, "Preparation of Barium Titanate Oxalate Tetrahydrate for Conversion to Barium Titanate of High Purity," *Journal of Research of the National Bureau of Standards*, vol. 56, 1956.
- [58] T. Yamamoto, K. Sanekika, and A. Yamamoto, "Preparation of thermostable and electric-conducting poly (2, 5-thienylene)," *Journal of Polymer Science: Polymer Letters Edition*, vol. 18, pp. 9-12, 1980.
- [59] J. W. P. Lin and L. P. Dudek, "Synthesis and properties of poly (2, 5-thienylene)," *Journal of Polymer Science: Polymer Chemistry Edition*, vol. 18, pp. 2869-2873, 1980.
- [60] K. Yoshino, S. Hayashi, and R.-i. Sugimoto, "Preparation and properties of conducting heterocyclic polymer films by chemical method," *Japanese Journal of Applied Physics*, vol. 23, p. L899, 1984.
- [61] S. J. Lee, J. M. Lee, I. W. Cheong, H. Lee, and J. H. Kim, "A facile route of polythiophene nanoparticles via Fe³⁺-catalyzed oxidative polymerization in aqueous medium," *Journal of Polymer Science Part A: Polymer Chemistry*, vol. 46, pp. 2097-2107, 2008.
- [62] H. Hamaker, "Formation of a deposit by electrophoresis," *Trans. Faraday Soc.*, vol. 35, pp. 279-287, 1940.
- [63] L. Besra and M. Liu, "A review on fundamentals and applications of electrophoretic deposition (EPD)," *Progress in materials science*, vol. 52, pp. 1-61, 2007.
- [64] M. Smoluchowski, "Versuch einer mathematischen Theorie der Koagulationskinetik kolloider Lösungen," 1917.
- [65] F. Bouyer and A. Foissy, "Electrophoretic deposition of silicon carbide," *Journal of the American Ceramic Society*, vol. 82, pp. 2001-2010, 1999.

- [66] D. Pavia, G. Lampman, G. Kriz, and J. Vyvyan, *Introduction to spectroscopy*: Cengage Learning, 2008.
- [67] B. D. Cullity and S. R. Stock, *Elements of X-ray Diffraction*: Pearson, 2001.
- [68] B. E. Warren, *X-ray Diffraction*: Courier Corporation, 1969.
- [69] D. C. Joy, "Scanning electron microscopy," *Materials Science and Technology*, 1971.
- [70] N. Unakar, J. Tsui, and C. Harding, "Scanning electron microscopy," *Ophthalmic Research*, vol. 13, pp. 20-35, 1981.
- [71] H. K. Wickramasinghe, "Scanning probe microscopy: Current status and future trends," *Journal of Vacuum Science & Technology A*, vol. 8, pp. 363-368, 1990.
- [72] G. Binnig, C. F. Quate, and C. Gerber, "Atomic force microscope," *Physical review letters*, vol. 56, p. 930, 1986.
- [73] A. Habib, R. Haubner, and N. Stelzer, "Effect of temperature, time and particle size of Ti precursor on hydrothermal synthesis of barium Titanate," *Materials Science and Engineering: B*, vol. 152, pp. 60-65, 2008.
- [74] X. G. Li, J. Li, and M. R. Huang, "Facile optimal synthesis of inherently electroconductive polythiophene nanoparticles," *Chemistry-A European Journal*, vol. 15, pp. 6446-6455, Jun 22 2009.
- [75] M. R. Karim, K. T. Lim, C. J. Lee, and M. S. Lee, "A facile synthesis of polythiophene nanowires," *Synthetic Metals*, vol. 157, pp. 1008-1012, 2007.
- [76] H. Wang, G. Tang, S. Jin, C. Bian, F. Han, D. Liang, *et al.*, "Effect of the preparation condition on the structure and conductive properties of polythiophene," *ACTA CHIMICA SINICA-CHINESE EDITION*-, vol. 65, p. 2454, 2007.
- [77] D. Damjanovic, "Ferroelectric, dielectric and piezoelectric properties of ferroelectric thin films and ceramics," *Reports on Progress in Physics*, vol. 61, p. 1267, 1998.